GENETICS, 2023, 223(4), iyad024
https://doi.org/10.1093/genetics/iyad024
Advance Access Publication Date: 16 February 2023
Fungal Genetics and Genomics

Parallel expansion and divergence of an adhesin family in pathogenic yeasts

Rachel A. Smoak,[1,†] Lindsey F. Snyder,[2,†] Jan S. Fassler,[2,3,*] Bin Z. He[2,3,*]

[1]Civil and Environmental Engineering, The University of Iowa, Iowa City, IA 52242, USA
[2]Interdisciplinary Graduate Program in Genetics, The University of Iowa, Iowa City, IA 52242, USA
[3]Department of Biology, The University of Iowa, Iowa City, IA 52242, USA

*Corresponding author: Email: bin-he@uiowa.edu (B.Z.H.); jan-fassler@uiowa.edu (J.S.F.)
[†]These authors contributed equally.

Abstract

Opportunistic yeast pathogens arose multiple times in the *Saccharomycetes* class, including the recently emerged, multidrug-resistant (MDR) *Candida auris*. We show that homologs of a known yeast adhesin family in *Candida albicans*, the Hyr/Iff-like (Hil) family, are enriched in distinct clades of *Candida* species as a result of multiple, independent expansions. Following gene duplication, the tandem repeat–rich region in these proteins diverged extremely rapidly and generated large variations in length and β-aggregation potential, both of which are known to directly affect adhesion. The conserved N-terminal effector domain was predicted to adopt a β-helical fold followed by an α-crystallin domain, making it structurally similar to a group of unrelated bacterial adhesins. Evolutionary analyses of the effector domain in *C. auris* revealed relaxed selective constraint combined with signatures of positive selection, suggesting functional diversification after gene duplication. Lastly, we found the Hil family genes to be enriched at chromosomal ends, which likely contributed to their expansion via ectopic recombination and break-induced replication. Combined, these results suggest that the expansion and diversification of adhesin families generate variation in adhesion and virulence within and between species and are a key step toward the emergence of fungal pathogens.

Keywords: *Candida auris*, adhesin, gene duplication, convergent evolution, opportunistic yeast pathogen, natural selection

Introduction

Candida auris, a newly emerged multidrug-resistant (MDR) yeast pathogen, is associated with a high mortality rate [up to 60% in a multicontinent meta-analysis (Lockhart *et al.* 2017)] and has caused multiple outbreaks across the world (CDC global *C. auris* cases count, 2021 February 15). As a result, it became the first fungal pathogen to be designated by CDC as an urgent threat (CDC 2019). The emergence of *C. auris* as a pathogen is part of a bigger evolutionary puzzle: *Candida* is a polyphyletic genus that contains most of the human yeast pathogens. Phylogenetically, species like *Candida albicans*, *C. auris*, and *Candida glabrata* belong to distinct clades with close relatives that either do not or only rarely infect humans (Fig. 1a). This strongly suggests that the ability to infect humans evolved multiple times in yeasts (Gabaldón *et al.* 2016). Because many of the newly emerged *Candida* pathogens are either resistant or can quickly evolve resistance to antifungal drugs (Lamoth *et al.* 2018; Srivastava *et al.* 2018), it is urgent to understand how yeast pathogenesis arose and what increases their survival in the host. We reason that any shared genetic changes among independently derived *Candida* pathogens will reveal key factors for host adaptation.

Gene duplication and the subsequent functional divergence are a major source for the evolution of novel phenotypes (Zhang 2003; Qian and Zhang 2014; Kuang *et al.* 2016; Eberlein *et al.* 2017). In a genome comparison of 7 pathogenic *Candida* species and 9 low pathogenic potential relatives, 3 of the top 6 pathogen-enriched gene families encode glycosylphosphatidylinositol (GPI)–anchored cell wall proteins, namely, Hyr/Iff-like (Hil), Als-like, and Pga30-like (Butler *et al.* 2009). The first two encode known fungal adhesins (Bailey *et al.* 1996; Hoyer 2001; Luo *et al.* 2010). These glycosylated cell wall proteins play key roles in fungal attachment to host endo- and epithelial cells, mediate biofilm formation and iron acquisition, and are well-established virulence factors (Hoyer *et al.* 2008; de Groot *et al.* 2013; Lipke 2018). It has been suggested that expansion of the cell wall protein repertoire, particularly adhesins, is a key step toward the evolution of yeast pathogens (Gabaldón *et al.* 2016). This is supported by a study showing that several adhesin families independently expanded in *C. glabrata* and close relatives (Gabaldón *et al.* 2013). Interestingly, studies of pathogenic *Escherichia coli* found that multiple strains independently acquired genes mediating intestinal adhesion, giving credence to the hypothesis from a different kingdom (Reid *et al.* 2000).

Despite the importance of adhesins in both the evolution and virulence of *Candida* pathogens, there is a lack of detailed phylogenetic analysis elucidating their evolutionary history (Hoyer 2001; Linder and Gustafsson 2008; Gabaldón *et al.* 2013). Even less is known about their sequence divergence and the role of natural selection in their evolution (Xie *et al.* 2011). In the newly emerged *C. auris*, individual adhesins have been characterized but there is little information about their evolutionary relationship

Received: December 07, 2022. **Accepted:** February 09, 2023

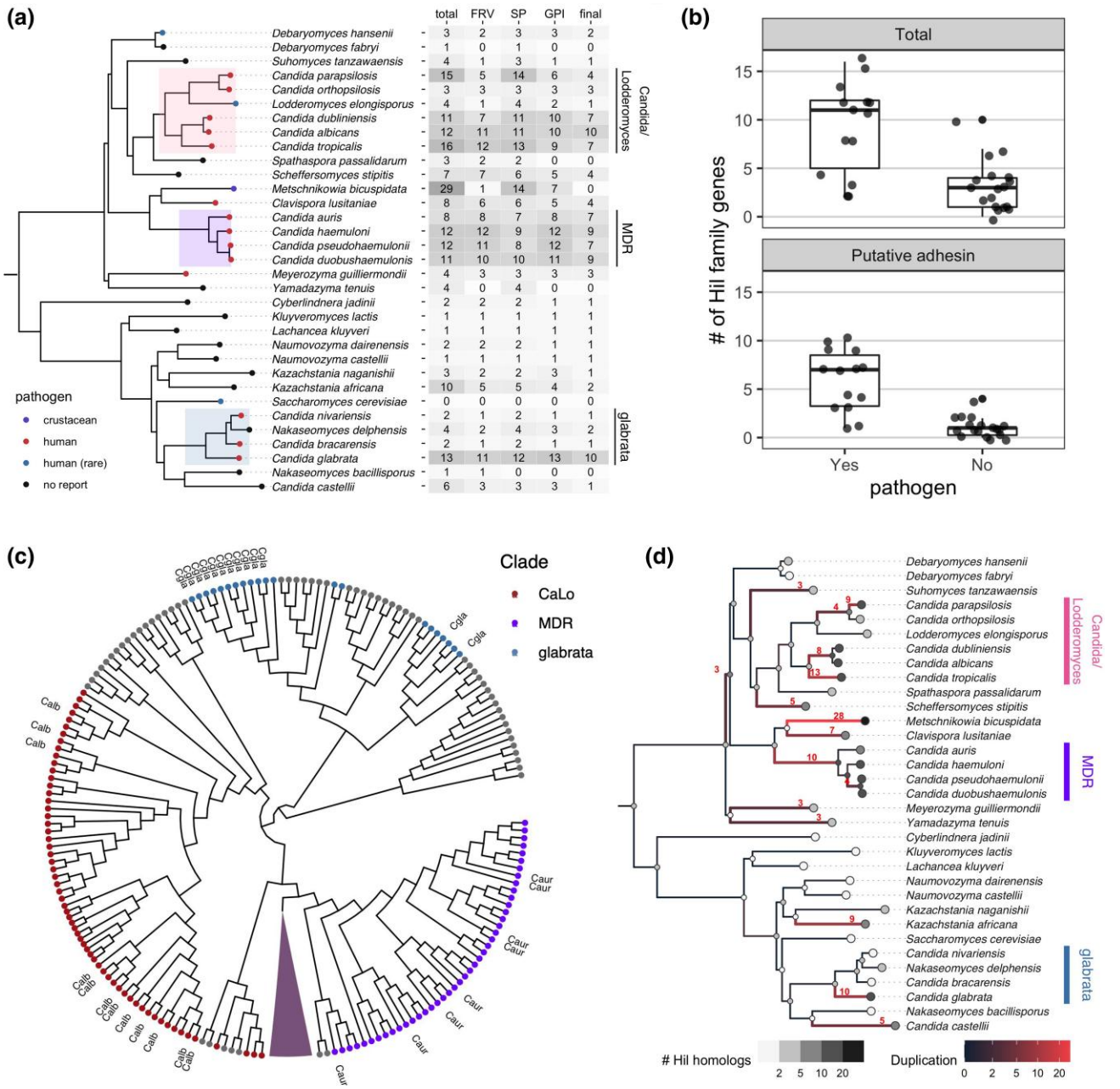

Fig. 1. Phylogenetic distribution of the yeast Hil family and its parallel expansion in independently derived pathogenic *Candida* species. a) Species tree is based on the phylogeny for 332 yeast species from Shen *et al.* (2018), except for 3 species in the MDR clade other than *C. auris*, whose phylogenetic relationships are based on Muñoz *et al.* (2018). The tip colors show the pathogenic status of the species. The highlighted clades are enriched in known human pathogens. In the table, the first column shows the total number of Hil family homologs per species. The number of homologs that pass each of the 3 tests for determining their adhesin status is shown in the next 3 columns. FRV: FungalRV, SP: signal peptide, and GPI: GPI anchor (see *Materials and methods* for details). The number of homologs passing all 3 tests is shown in the "final" columns. b) Boxplots comparing the number of Hil homologs (upper) or the number of putative adhesins passing all 3 tests (lower) per species between known pathogens and low pathogenic potential species. Individual species numbers are shown as dots on top of the boxplot. Homologs from *M. bicuspidata* were excluded (see text). Both comparisons are significant at a 0.005 level by either a *t*-test with unequal variance or Mann–Whitney *U* test. c) Maximum likelihood tree based on the Hyphal_reg_CWP domain of the Hil family was shown as a cladogram. All 29 homologs in *M. bicuspidata* formed a single group, which is shown as a triangle. Homologs from the species in the 3 highlighted clades in (A) are colored accordingly. CaLo: Candida/Lodderomyces. Homologs from *C. albicans*, *C. auris*, and *C. glabrata* are labeled as Calb, Caur, and Cgla, respectively. d) Species tree showing the number of inferred duplication events on each branch. The shading of the tip and internal nodes represent the identified and inferred number of Hil homologs, respectively. The branch color shows the inferred number of duplication events, with 3 or more duplications also shown as a number next to the branch.

with homologs in other *Candida* species and how their sequences diverged (Kean *et al.* 2018; Singh *et al.* 2019; Muñoz *et al.* 2021). In this study, we characterized the detailed evolutionary history of a yeast adhesin family and used *C. auris* as a focal group to determine how adhesin sequences diverged under various natural selection forces. To choose a candidate adhesin family in *C. auris*, we compared it with the well-studied *C. albicans*, which belongs to the same CUG-Ser1 clade. Of the known adhesins in *C. albicans*, *C. auris* lacks the Hwp family and has only 3 Als or Als-like proteins compared with 8 Als proteins in *C. albicans* (Muñoz *et al.* 2018). By

Table 1. Software and algorithm list.

Name	Reference	Web or download URL
AlphaFold2	Jumper *et al.* (2021)	https://github.com/sokrypton/ColabFold (links to DeepMind Google Colab Notebook)
BLAST + v2.12.0	Camacho *et al.* (2009)	https://blast.ncbi.nlm.nih.gov/
ClipKit	Steenwyk *et al.* (2020)	https://github.com/JLSteenwyk/ClipKIT
Clustal Omega v1.2.4	Sievers *et al.* (2011)	http://www.clustal.org/omega/
Custom R, Python, and shell scripts	This study	https://github.com/binhe-lab/C037-Cand-auris-adhesin
DALI	Holm (2022)	http://ekhidna2.biocenter.helsinki.fi/dali/
EMBOSS v6.6.0.0	Rice *et al.* (2000)	http://emboss.open-bio.org/
FungalRV	Chaudhuri *et al.* (2011)	http://fungalrv.igib.res.in/
GeneRax v2.0.1	Morel *et al.* (2020)	https://github.com/BenoitMorel/GeneRax
HmmerWeb (hmmscan)	Potter *et al.* (2018)	https://www.ebi.ac.uk/Tools/hmmer/search/hmmscan
I-TASSER	Yang *et al.* (2015)	https://zhanggroup.org/I-TASSER/
Jalview v2.11	Waterhouse *et al.* (2009)	https://www.jalview.org/
JDotter	Brodie *et al.* (2004)	https://4virology.net/virology-ca-tools/jdotter/
NetNGlyc v1.0	Gupta and Brunak (2002)	https://services.healthtech.dtu.dk/service.php?NetNGlyc-1.0
NetOGlyc v4.0	Steentoft *et al.* (2013)	https://services.healthtech.dtu.dk/service.php?NetOGlyc-4.0
PAL2NAL.pl	Suyama *et al.* (2006)	http://www.bork.embl.de/pal2nal/
PAML v4.9e	Yang (2007)	http://abacus.gene.ucl.ac.uk/software/paml.html
pDOMTHREADER	Lobley *et al.* (2009)	http://bioinf.cs.ucl.ac.uk/psipred/psiform.html
PredGPI	Pierleoni *et al.* (2008)	http://gpcr.biocomp.unibo.it/predgpi/
PSIPred	Buchan and Jones (2019)	http://bioinf.cs.ucl.ac.uk/psipred/
PyMol v2.5.2	Schrödinger, LLC (2021)	https://pymol.org/
R package—ggtree v3.2.1	Yu (2020)	https://github.com/YuLab-SMU/ggtree
R package—phylolm	Ho et al. (2014)	https://cran.r-project.org/web/packages/phylolm/index.html
R package—rentrez v1.2.3	Winter (2017)	https://github.com/ropensci/rentrez
R package—treeio v1.18.1	Wang *et al.* (2020)	https://github.com/YuLab-SMU/treeio
R v4.1.0	(R Core Team)	https://cran.r-project.org/
RAxML v8.0.0	Stamatakis (2014)	https://cme.h-its.org/exelixis/web/software/raxml/
RAxML-NG v1.1.0	Kozlov *et al.* (2019)	https://github.com/amkozlov/raxml-ng
RStudio v1.4	RStudio Team (2021)	https://www.rstudio.com/
SignalP 6.0	Teufel *et al.* (2022)	http://www.cbs.dtu.dk/services/SignalP/
TANGO v2.3.1	Fernandez-Escamilla *et al.* (2004)	http://tango.crg.es/
XSTREAM	Newman and Cooper (2007)	https://amnewmanlab.stanford.edu/xstream/download.jsp

contrast, *C. auris* has 8 genes with a Hyphal_reg_CWP (PF11765) domain found in the Hyr/Iff family in *C. albicans* (Muñoz *et al.* 2021). This family was one of the most highly enriched in pathogenic *Candida* species relative to nonpathogenic ones (Butler *et al.* 2009). Transcriptomic studies identified two *C. auris HIL* genes as being upregulated during biofilm formation and under antifungal treatment (Kean *et al.* 2018). Interestingly, isolates from the less virulent *C. auris* Clade II lack 5 of the 8 *HIL* genes (Muñoz *et al.* 2021). It is currently not known whether the *C. auris HIL* genes encode adhesins, how they relate to the *C. albicans* Hyr/Iff family genes, and how their sequences diverged after duplication.

We show that the Hil family independently expanded multiple times, including in *C. auris* and *C. albicans*. Using *C. auris* as a focal species, we show in detail how sequence features and predicted structures of the effector domain offer support for the hypothesis that its Hil family members encode adhesins, while rates of nonsynonymous to synonymous substitutions reveal varying strengths of selective constraint and positive selection acting on the effector domain during the expansion of the family. The observed pattern of rapid divergence in the repeat-rich central domain was found to be general across the entire family and led to large variations in length and β-aggregation potential both between and within species, likely contributing to phenotypic diversity in adhesion and virulence.

Materials and methods

Software

Versions and sources of the main software used in this study are listed in Table 1.

Identify Hil family homologs in yeasts and beyond

To identify the Hil family proteins in yeasts and beyond, we used the Hyphal_reg_CWP domain sequence from 3 distantly related Hil homologs as queries, namely, *C. albicans* Hyr1 (XP_722183.2), *C. auris* Hil1 (XP_028889033), and *C. glabrata* CAGL0E06600g (XP_722183.2). We performed BLASTP searches in the RefSeq protein database with an *E*-value cut-off of 1×10^{-5}, with a minimum query coverage of 50%, and with the low-complexity filter on. All hits were from Ascomycota (yeasts), and all but one were from the Saccharomycetes class (budding yeast). A single hit was found in the fission yeast *Schizosaccharomyces cryophilus*. Using that hit as the query, we searched all fission yeasts in the nr protein database, with a relaxed *E*-value cut-off of 10^{-3}, and identified no additional hits. We thus excluded that one hit from downstream analyses. To supplement the RefSeq database, which lacks some yeast species such as those in the Nakaseomyces genus, we searched the Genome Resources for Yeast Chromosomes (GRYC, http://gryc.inra.fr/). Using the same criteria, we recovered 16 additional sequences. To allow for gene tree and species tree reconciliation, we excluded 3 species that are not part of the 322 species yeast phylogeny (Shen *et al.* 2018) and not a member of the MDR clade (Muñoz *et al.* 2018). Further details, including additional quality control steps taken to ensure that the homolog sequences are accurate and complete, can be found in Supplementary Text 1. In total, we curated a list of 215 Hil family homologs from 32 species.

Gene family enrichment analysis

To determine if the Hil family is enriched in the pathogenic yeasts, we performed 2 analyses. In the first analysis, we divided the

species into pathogens vs low pathogenic potential groups and performed a *t*-test with unequal variance (also known as Welch's test) as well as a nonparametric Mann–Whitney *U* test to compare the Hil family size in the 2 groups. For both tests, we used either the total size of the family or the number of putative adhesins as the random variable, and the results were consistent. We excluded homologs from *Metschnikowia bicuspidata* because 10 of its 29 Hil family proteins were annotated as incomplete in the RefSeq protein database and also because as a parasite of freshwater crustaceans, it does not fit into either the human pathogen or the low pathogenic potential group. *Saccharomyces cerevisiae* was included in the comparison as an example of species with zero members of the Hil family. We chose *S. cerevisiae* because we could be confident about its lack of a Hil family homolog thanks to its well-assembled and well-annotated genome.

In the second test, we used phylogenetic logistic regression (Ives and Garland 2010) to account for the phylogenetic relatedness between species. We used the "phyloglm" function in the "phylolm" package in R, with {method = "logistic_IG10," btol = 50, boot = 100}. The species tree, including the topology and branch lengths, were based on the 322 species phylogeny from Shen *et al.* (2018), supplemented by the phylogenetic relationship for the MDR clade based on Muñoz *et al.* (2018). The *P*-values based on phylogenetically specified residual correlations were reported.

Phylogenetic analysis of the Hil family and inference of gene duplications and losses

To infer the evolutionary history of the Hil family, we reconstructed a maximum likelihood tree based on the alignment of the Hyphal_reg_CWP domain. First, we used hmmscan (HmmerWeb version 2.41.2) to identify the location of the Hyphal_reg_CWP domain in each Hil homolog. We used the "envelope boundaries" to define the domain in each sequence and then aligned their amino acid sequences using Clustal Omega with the parameter {–iter = 5}. We then trimmed the alignment using ClipKit with its default smart-gap trimming mode (Steenwyk *et al.* 2020). RAxML-NG v1.1.0 was run in the MPI mode with the following parameters on the alignment: "raxml-ng-mpi –all –msa INPUT –model LG + G –seed 123 –bs-trees autoMRE." The resulting tree was corrected using GeneRax, which seeks to maximize the joint likelihood of observing the alignment given the gene family tree (GFT) and observing the GFT given the species phylogeny, using the parameter {–rec-model UndatedDL}. The species tree used is the same as the one used for the phylogenetic logistic regression above. In addition to correcting the GFT, GeneRax also reconciled it with the species tree and inferred duplication and loss event counts on each branch. Tree annotation and visualization were done in R using the treeio and ggtree packages (Yu 2020; Wang *et al.* 2020).

To infer the phylogenetic tree for the Hil family homologs in various *C. auris* strains and infer gains and losses within species, we identified orthologs of the *HIL* genes in representative strains from the 4 major clades of *C. auris* (B8441, B11220, B11221, B11243) (Muñoz *et al.* 2018). Orthologs from 2 MDR species, *Candida haemulonii* and *Candida pseudohaemulonis*, and from *Debaryomyces hansenii* were included to help root the tree. The gene tree was constructed as described above. To root the tree, we first inferred a gene tree without the outgroup (*D. hansenii*) sequences in the alignment. Then, the full alignment with the outgroup sequences along with the gene tree from the first step were provided to RAxML to run the Evolutionary Placement Algorithm (EPA) algorithm (Berger *et al.* 2011), which identified a unique root location. To reconcile the gene tree with the species tree, we performed maximum likelihood–based gene tree correction using GeneRax (v2.0.1) with the following parameters: {–rec-model UndatedDL}. The species tree was based on Muñoz *et al.* (2018).

Prediction for fungal adhesins and adhesin-related sequence features

(1) The potential of Hil homologs encoding fungal adhesins was assessed using FungalRV, a support vector machine–based fungal adhesin predictor (Chaudhuri *et al.* 2011). Proteins passing the recommended cut-off of 0.511 were considered positive. (2) Signal peptide was predicted using the SignalP 6.0 server, with the "organism group" set to Eukarya. The server reported the proteins that had predicted signal peptides. No further filtering was done. (3) GPI anchor was predicted using PredGPI using the general model. Proteins with a false-positive rate of 0.01 or less were considered as containing a GPI anchor. (4) Tandem repeats were identified using XSTREAM with the following parameters: {-i.7 -I.7 -g3 -e2 -L15 -z -Asub.txt -B -O}, where the "sub.txt" was provided by the software package. (5) β-aggregation–prone sequences were predicted using TANGO v2.3.1 with the following parameters: {ct="N" nt="N" ph="7.5" te="298" io="0.1" tf="0" stab="−10" conc="1" seq="SEQ"}. (6) Serine and threonine content in proteins were quantified using "freak" from the EMBOSS suite, with a sliding window of 100 or 50 aa and a step size of 10 aa. To compare with proteome-wide distribution of Ser/Thr frequency, the protein sequences for *C. albicans* (SC5314), *C. glabrata* (CBS138), and *C. auris* (B11221) were downloaded from NCBI Assembly database (IDs in Supplementary Table 7) and the frequency of serine and threonine residues was counted for each protein. (7) O-linked and N-linked glycosylations were predicted using NetOGlyc (v4.0) and NetNGlyc (v1.0) servers.

Structural prediction and visualization for the Hyphal_reg_CWP domain

To perform structural predictions using AlphaFold2, we used the Google Colab notebook (https://colab.research.google.com/github/deepmind/alphafold/blob/main/notebooks/AlphaFold.ipynb) authored by the DeepMind team. This is a reduced version of the full AlphaFold version 2 in that it searches a selected portion of the environmental BFD database and does not use templates. The Amber relaxation step is included, and no other parameters other than the input sequences are required. DALI was used to search for similar structures in the PDB50 database. Model visualization and annotation were done in PyMol v2.5.2. Secondary structure prediction for *C. auris* Hil1's central domain was performed using PSIPred.

Dotplot

To determine the self-similarity and similarity between the 8 *C. auris* Hil proteins, we made dotplots using JDotter (Brodie *et al.* 2004). The window size and contrast settings were labeled in the legends for the respective plots. The self-alignment for *C. auris* Hil1 tandem repeats was visualized using Jalview v2.11.

Identification of intraspecific tandem repeat copy number variations among *C. auris* strains

To identify polymorphisms in Hil1–Hil4 in diverse *C. auris* strains, we downloaded the genome sequences for the following strains from NCBI: Clade I, B11205 and B13916; Clade II, B11220, B12043, and B13463; Clade III, B11221, B12037, B12631, and B17721; and Clade IV, B11245 and B12342 (Supplementary Table 4). The amino acid sequences for Hil1–Hil4 from the strain B8441 were used as

the query to search the nucleotide sequences of the above assemblies using TBLASTN, with the following parameters {-db_gencode 12 -evalue 1e-150 -max_hsps 2}. Orthologs in each strain were curated based on the BLAST hits to either the Hyphal_reg_CWP domain alone or the entire protein query. All Clade II strains had no hits for Hil1–Hil4. Several strains in Clades I, III, and IV were found to lack one or more Hil proteins (Supplementary Table 5). But upon further inspection, it was found that they had significant TBLASTN hits for part of the query, e.g. the central domain, and the hits were located at the end of a chromosome, suggesting the possibility of incomplete or misassembled sequences. Further experiments will be needed to determine if those *HIL* genes are present in those strains.

Estimation of dN/dS ratios and model comparisons

We used "codeml" in PAML (v4.9e) to perform evolutionary inferences on the Hyphal_reg_CWP domain in *C. auris*. We first used Clustal Omega to align the amino acid sequences for the Hyphal_reg_CWP domain from Hil1–Hil8 from *C. auris* similar to how we generated the multiple sequence alignment for all Hil proteins. A closely related outgroup (XP_018709340.1 from *M. bicuspidata*) was included to root the tree. We then generated a coding sequence alignment from the protein alignment using PAL2NAL (Suyama *et al.* 2006). We used GARD (Kosakovsky Pond *et al.* 2006) to analyze the coding sequence alignment to detect gene conversion events. The web service of GARD on datamonkey.org was run with the following parameters: {data type: nucleotide, run mode: normal, genetic code: yeast alternative nuclear, site-to-site rate variation: general discrete, rate classes: 3}. Based on the results, we identified 2 putatively nonrecombining partitions, P1 = 1–414 and P2 = 697–981 (the numbers refer to the alignment columns). We then separately analyzed the 2 partitions in PAML. To test hypotheses about positive selection on a subset of the sites on all branches, we compared models M2a vs M1a, M8 vs M7, and M8a vs M8. The first 4 models were specified by {seqtype = 1, CodonFreq = 1, model = 0, NSsites = 0,1,2,7,8, icode = 8, fix_kappa = 0, kappa = 2, fix_omega = 0, omega = 0.4, cleandata = 1}. The model M8a is additionally specified by { seqtype = 1, CodonFreq = 1, model = 0, NSsites = 8, fix_omega = 1 and omega = 1, cleandata = 1}. To test hypotheses for variable dN/dS on different branches (no variation across sites), we used {model = 0 or 1 or 2, NSsites = 0}, with the rest being the same as the site tests. Model = 0 specified the single-ratio model, model = 1 the free-ratio model, and model = 2 the user-defined model. For the user-defined model, we first used estimates from the free-ratio model to designate a set of branches with dN/dS > 10 as the foreground and then tested if their dN/dS was significantly different from the rest of the tree by comparing a 2-ratio model with the single-ratio model. Since the results were significant, we further tested if the foreground dN/dS was significantly greater than 1, by comparing the 2-ratio model to a constrained version of the model where omega was fixed at 1. For branch-site test, we used {model = 2, NSsites = 2, fix_omega = 0, omega = .4} as the alternative model and {model = 2, NSsites = 2, fix_omega = 1, omega = 1} as the null to test for positive selection on a subset of the sites on the foreground branches. Sites under positive selection were identified using the Bayes Empirical Bayes (BEB) procedure, with a posterior probability threshold of 0.99.

Chromosomal locations of Hil family genes

To compare the chromosomal locations of the Hil family genes to the background distribution, we selected 8 species whose genomes were assembled to a chromosomal level and are not within a closely related group, including *C. albicans*, *D. hansenii*, *Candida orthopsilosis*, *Kazachstania africana*, *Kluyveromyces lactis*, *Naumovozyma dairenensis*, *C. auris*, and *C. glabrata* (Supplementary Table 7). We did not include some species, e.g. *Candida dubliniensis*, to minimize statistical dependence due to shared ancestry. The RefSeq assembly for *C. auris* was included even though it was at a scaffold level because a recent study showed that 7 of its longest scaffolds were chromosome-length, allowing the mapping of the scaffolds to chromosomes (Muñoz *et al.* 2021, supplementary table 1). To determine the chromosomal locations of the Hil homologs in these 8 species, we used Rentrez v1.2.3 (Winter 2017) in R to retrieve their chromosome ID and coordinates. To calculate the background gene density on each chromosome, we downloaded the feature tables for the 8 assemblies from the NCBI assembly database and calculated the location of each gene as its start coordinate divided by the chromosome length. To compare the chromosomal location of the Hil family genes to the genome background, we divided each chromosome into 5 equal-sized bins based on the physical distance to the nearest chromosomal end. We calculated the proportion of genes residing in each bin for the Hil family or for all protein-coding genes. To determine if the 2 distributions differ significantly from 1 another, we performed a goodness-of-fit test using either a log–likelihood ratio (LLR) test or a chi-squared test, as implemented in the XNomial package in R (Engels 2015). The LLR test *P*-value was reported.

Results

Phylogenetic distribution of the Hil family and its potential to encode adhesin

The Hyr/Iff family was first identified and characterized in *C. albicans* (Bailey *et al.* 1996; Richard and Plaine 2007). The family is defined by its N-terminal hyphally regulated cell wall protein domain (Hyphal_reg_CWP, PF11765), followed by a highly variable central domain rich in tandem repeats (Boisramé *et al.* 2011). Because the effector domain is more conserved than the repeat region and plays a prominent role in mediating adhesion in known yeast adhesins (Willaert 2018), here, we define the Hil family as the group of evolutionarily related proteins sharing the Hyphal_reg_CWP domain, different from a previous definition based on sequence similarity in either the Hyphal_reg_CWP domain or the repeat region (Butler *et al.* 2009).

To determine the phylogenetic distribution of the Hil family and its association with the pathogenic potential of species, we performed BLASTP searches using the Hyphal_reg_CWP domain from 3 distantly related Hil homologs as queries (from *C. auris*, *C. albicans*, and *C. glabrata*). We scrutinized the database hits and searched additional assemblies to ensure that their sequences are complete and accurate given the available genome assemblies (Supplementary Text 1). Using the criteria of *E*-value < 10^{-5} and query coverage > 50%, we identified a total of 215 proteins containing the Hyphal_reg_CWP domain from 32 species (Fig. 1a, Supplementary Table 1). No credible hits were identified outside the budding yeast subphylum even after a lower *E*-value cut-off of 10^{-3} was tested, suggesting that this family is specific to this group (see *Materials and Methods*). Species with 8 or more Hil family genes fell largely within the multidrug resistant (MDR) and the Candida/Lodderomyces (CaLo) clades, which include *C. auris* and *C. albicans*, respectively. Only 3 such species were found outside of the 2 clades: *C. glabrata*, *M. bicuspidata*, and *K. africana*. *C. glabrata* is a major opportunistic pathogen that is more closely related to *S. cerevisiae* than to most other

Candida species (Dujon *et al.* 2004; Butler *et al.* 2009; Gabaldón *et al.* 2013). *M. bicuspidata* is part of the CUG-Ser1 clade. While not a pathogen in humans, it is a parasite of freshwater animals (Hall *et al.* 2010; Jiang *et al.* 2022). *K. africana* is not closely related to any known yeast pathogen, and its ecology is poorly understood (Gordon *et al.* 2011).

We then asked how many of the Hil family genes in each species are likely to encode yeast adhesins. To get an initial estimate, we combined a machine learning tool for predicting fungal adhesins (Chaudhuri *et al.* 2011) with predictions for the N-terminal signal peptide and C-terminal GPI anchor sequence, 2 features shared by the majority of known fungal adhesins (Lipke 2018). Half of all Hil homologs passed all 3 tests (Fig. 1a). Notably, *M. bicuspidata* has the largest Hil family among all species, but none of its 29 Hil genes passed all tests. We found most of the identified hits in this species were short relative to the rest of the family (Supplementary Fig. 1), and 10 of the 29 hits were annotated as being incomplete in the RefSeq database. Further analyses with a better assembled genome and functional studies are needed to determine if the Hil family in this species has unique properties and functions.

Independent expansion of the Hil family in multiple pathogenic *Candida* lineages

Pathogenic yeast species have on average a larger Hil family, and also, more of its members were predicted to encode adhesins than in low pathogenic potential species (Fig. 1b, *t*-test with unequal variance and Mann–Whitney *U* test both yielded $P < 0.005$, one-sided test). This naive comparison does not account for phylogenetic relatedness between species and could result in a false-positive association (Levy *et al.* 2018; Bradley *et al.* 2018). To address this, we performed phylogenetic logistic regression, which uses the known phylogeny to specify the residual correlation structure among species with shared ancestry (Ives and Garland 2010). We tested for associations between the pathogen status with either the total number of Hil homologs or the number of putative adhesins in each species. Both tests were significant ($P = 0.005$ and 0.007, respectively). Together, these results strongly support an enrichment of the Hil family and the putative adhesins therein among the pathogenic yeast species.

Some adhesin families have undergone independent expansions even among closely related species (Gabaldón *et al.* 2013). This would result in overestimation of the phylogenetic signal in the above analysis. To further characterize the evolutionary history of the Hil family, including among closely related *Candida* lineages, we reconstructed a species tree–aware maximum likelihood phylogeny for the Hil family based on the Hyphal_reg_CWP domain alignment (Fig. 1c, Supplementary Fig. 2). We found that homologs from the MDR clade and the CaLo clade separated into 2 groups, suggesting that the duplications of the Hil family genes in the 2 clades occurred independently. To better illustrate the history of gene duplications in the Hil family, we reconciled the gene tree with the species tree and mapped the number of duplications onto the species phylogeny (see *Materials and Methods*). The result showed that the Hil family has independently expanded multiple times, not only between clades but also among closely related species within a clade, such as in *C. albicans* and *C. tropicalis* (Fig. 1d).

Sequence features of the *C. auris* Hil family support their adhesin status

Experiments have demonstrated that Hil family members function as adhesin in *C. albicans* and more recently for one member in *C. glabrata* (Bailey *et al.* 1996; Boisramé *et al.* 2011; Rosiana *et al.* 2021; Reithofer *et al.* 2021). To further evaluate the adhesin function of Hil family proteins, we focused on *C. auris*, in which Hil family members were implicated in biofilm formation and response to antifungal treatments but still remain poorly characterized (Kean *et al.* 2018). We named the 8 *C. auris* Hil family proteins Hil1–Hil8 ordered by their length (Supplementary Table 2). This differs from the literature, which referred to them by their most closely related Hyr/Iff genes in *C. albicans* (Kean *et al.* 2018; Jenull *et al.* 2021; Muñoz *et al.* 2021). The renaming avoids the incorrect implication of one-to-one orthology between the 2 species (Fig. 1c).

To further assess the adhesin potential for the *C. auris* Hil family, we compared their domain architecture and sequence features to those typical of known yeast adhesins, including a signal peptide, an effector domain, a Ser/Thr-rich and highly glycosylated central domain with tandem repeats and β-aggregation–prone sequences, and a GPI anchor signal (Fig. 2a) (de Groot *et al.* 2013; Lipke 2018). All 8 *C. auris* Hil proteins followed this domain architecture (Fig. 2b). Hil1–4 were additionally characterized by an array of regularly spaced β-aggregation–prone sequences (red ticks below the protein, Fig. 2b). All 8 proteins also had elevated Ser/Thr frequencies in their central domain and were predicted to be heavily O-glycosylated (Fig. 2c). Predicted N-glycosylation was rare except in Hil5 and Hil6 (Fig. 2c). The overall Ser/Thr frequencies in the Hil family proteins were significantly elevated compared with the rest of the proteome (Supplementary Fig. 3). All 8 members were predicted to be fungal adhesins by FungalRV, a support vector machine–based classifier that showed high sensitivity and specificity in 8 pathogenic fungi based on sequence features (Chaudhuri *et al.* 2011).

Hyphal_reg_CWP domain in the Hil family is predicted to adopt a β-helical fold similar to unrelated bacterial adhesin binding domains

Crystal structures of the effector domain in several yeast adhesin families, including Als, Epa, and Flo, revealed carbohydrate- or peptide-binding activities supporting the proteins' adhesin functions (Willaert 2018). The structure of the Hyphal_reg_CWP domain in the Hil family in this study has not yet been experimentally determined. However, crystal structures for the effector domains of 2 adhesin-like wall proteins (Awp1 and Awp3b) in *C. glabrata*, which are distantly related to those in the Hil family, were recently reported, and the predicted structure of 1 of *C. glabrata*'s Hil family members (Awp2) was found to be highly similar to the 2 solved structures (Reithofer *et al.* 2021). We used AlphaFold2 (Jumper *et al.* 2021) to predict the structures of the effector domain for 2 *C. auris* Hil proteins, Hil1 and Hil7 (Fig. 3, a and b). Both resemble the *C. glabrata* Awp1 effector domain (Fig. 3c), consisting of a right-handed β-helix at the N-terminus followed by an α-crystallin fold. There are 3 β-strands in each of the 9 rungs in the β-helix, stacked into 3 parallel β-sheets (Fig. 3d). The α-crystallin domain consists of 7 β-strands forming 2 antiparallel β-sheets, adopting an immunoglobulin-like β-sandwich fold (Fig. 3e) (Koteiche and Mchaourab 1999; Stamler *et al.* 2005).

The β-strand–rich structure is typical of effector domains in known yeast adhesins, but the β-helix fold at the N-terminus is uncommon (Willaert 2018). Proteins with a β-helix domain often have carbohydrate-binding capabilities and act as enzymes, e.g. hydrolase and pectate lyase (SCOP ID: 3001746). To gain further insight into Hyphal_reg_CWP domain's function, we searched the PDB50 database for structures similar to what was predicted for *C. auris* Hil1 using DALI (Holm 2022). We identified a number

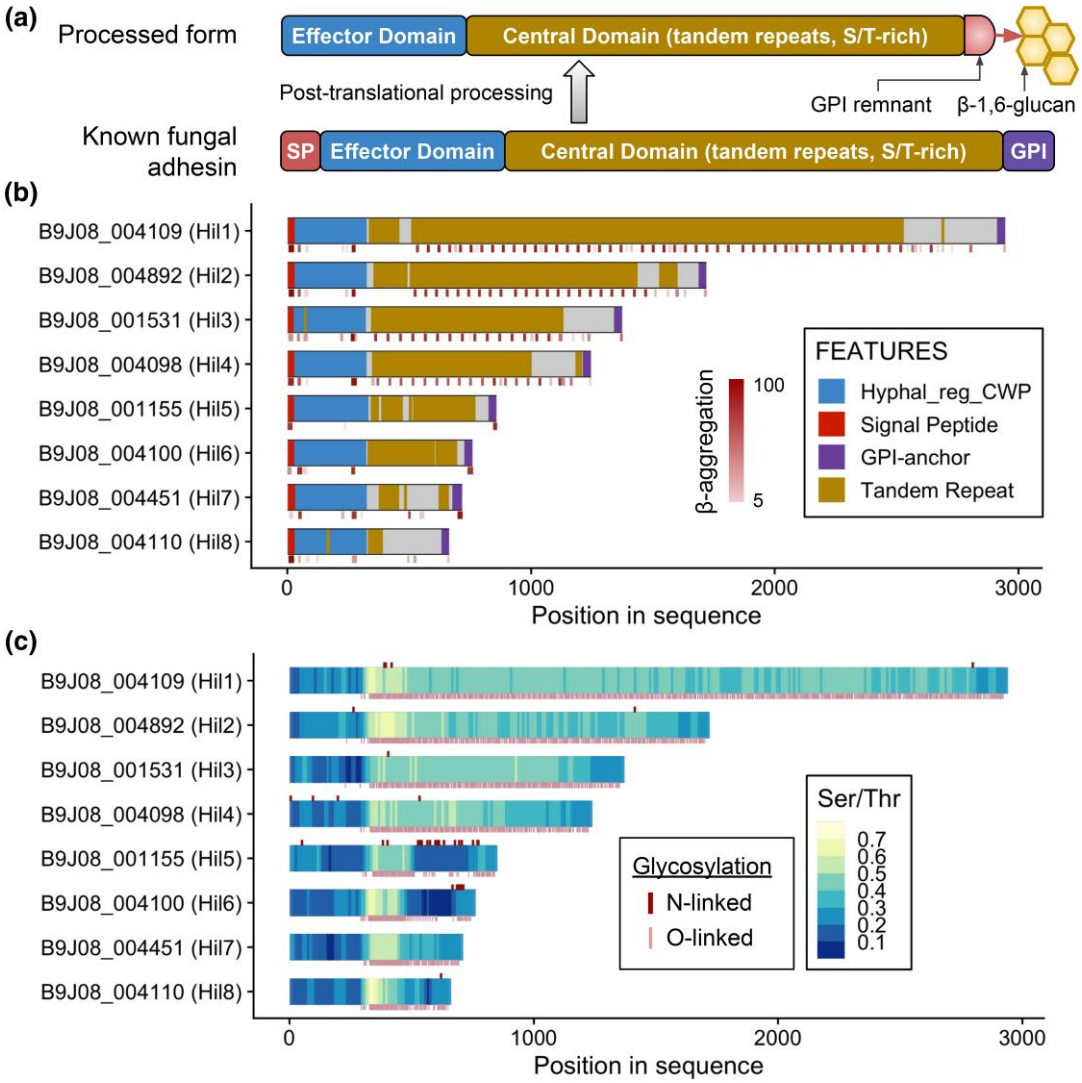

Fig. 2. Domain architecture and adhesin-associated features of the *C. auris* Hil family. a) Diagram depicting the domain organization of a typical yeast adhesin before and after the posttranslational processing, adapted from de Groot *et al.* (2013). b) Domain features of the 8 Hil proteins in *C. auris* (strain B8441). Gene IDs and names are labeled on the left. The short stripes below each diagram are the TANGO-predicted β-aggregation–prone sequences, with the intensity of the color corresponding to the score of the prediction. c) Serine and threonine (Ser/Thr) frequencies in each protein are plotted in 50 aa sliding windows with step size of 10 aa. N-linked and O-linked glycosylation sites were predicted by NetNGlyc 1.0 and NetOGlyc 4.0, respectively, and are shown as short ticks above and below each protein schematic.

of bacterial adhesins with a highly similar β-helix fold but no α-crystallin domain (Supplementary Table 3), e.g. Hmw1 from *Haemophilus influenzae* (PDB: 2ODL), tāpirins from *Caldicellulosiruptor hydrothermalis* (PDB: 6N2C), TibA from enterotoxigenic *E. coli* (PDB: 4Q1Q), and SRRP from *Limosilactobacillus reuteri* (PDB: 5NY0). For comparison, the binding region of the serine-rich repeat protein 100-23 ($SRRP_{100\text{-}23}$) from *L. reuteri* was shown in Fig. 3f (Sequeira *et al.* 2018). Together, these results strongly suggest that the Hyphal_reg_CWP domain in the *C. auris* Hil family genes mediates adhesion. Additionally, the low sequence identity (12–15%) between the yeast Hyphal_reg_CWP domain and the bacterial adhesins' binding regions further suggests the 2 groups have convergently evolved a similar structure to achieve adhesion functions.

Rapid divergence of the repeat-rich central domain in Hil family proteins in *C. auris*

While the overall domain architecture is well conserved, the 8 Hil family proteins in *C. auris* differ significantly in length and sequence of their central domains (Fig. 2b). While not involved in ligand binding, central domains in yeast adhesins are known to play a critical role in mediating adhesion: the length and stiffness of the central domain are essential for elevating and exposing the effector domain (Frieman *et al.* 2002; Boisramé *et al.* 2011), and the tandem repeats and β-aggregation sequences within them directly contribute to adhesion by mediating homophilic binding and amyloid formation (Rauceo *et al.* 2006; Otoo *et al.* 2008; Frank *et al.* 2010; Wilkins *et al.* 2018). Thus, divergence in the central domain of the Hil family has the potential to lead to phenotypic diversity, as shown in *S. cerevisiae* (Verstrepen *et al.* 2004, 2005).

To determine how the central domain sequences evolved in the *C. auris* Hil family, we used dot plots both to reveal the tandem repeat structure within each protein and to examine the similarity among the paralogs. A "dot" on the x–y plot indicates that the corresponding segments (window size = 50 a.a.) from the 2 proteins on the x- and y-axes share similarity, with the gray scale being proportional to the degree of similarity (Brodie *et al.* 2004). We found that *C. auris* Hil1, Hil2, Hil3, and Hil4 share a ~44 aa repeat

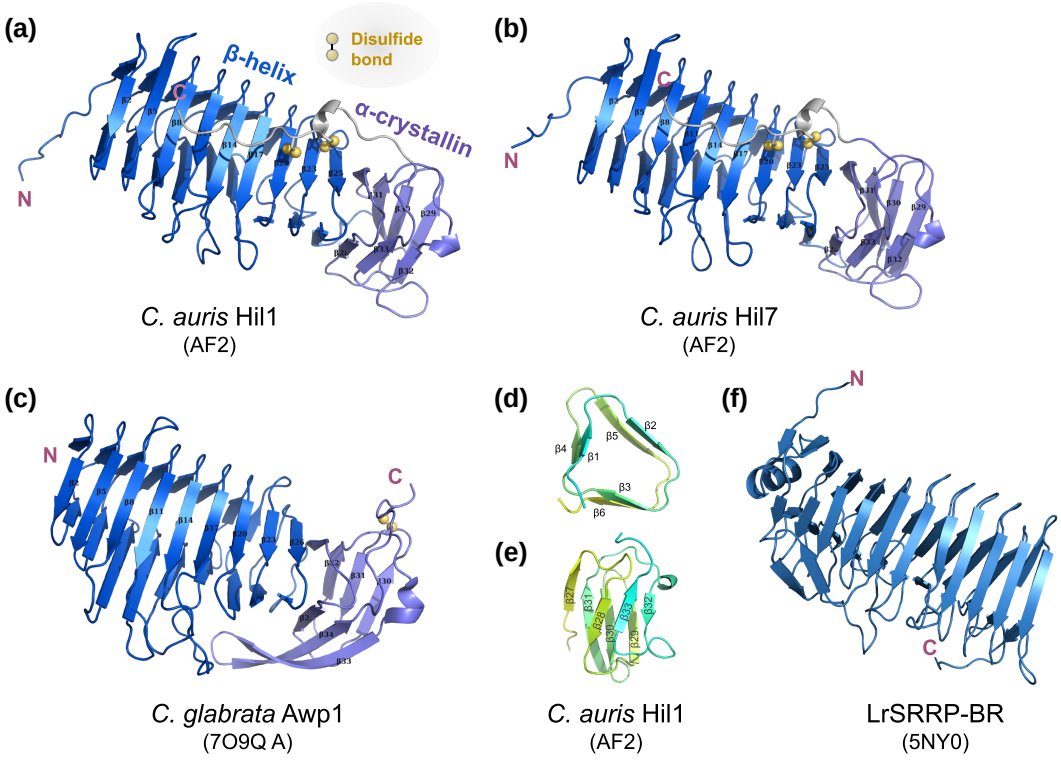

Fig. 3. Predicted structures of the Hyphal_reg_CWP domain in 2 *C. auris* Hil proteins are similar to yeast and bacterial adhesins. a) and (b) AlphaFold2 (AF2)–predicted structures of the Hyphal_reg_CWP domains from *C. auris* Hil1 and Hil7, which consist of a β-helix followed by a α-crystallin domain, with the C-terminal loop linked to the β-helix via 2 disulfide bonds. c) Crystal structure of the *C. glabrata* Awp1 effector domain, which is highly similar to *C. auris* Hil1 and Hil7, but with the disulfide bond in a different location. d) Cross-section of the first 2 rungs of the β-helix in (a), showing the 3 β-strands per rung. e) α-Crystallin domain in (a), showing the 7 β-strands forming 2 antiparallel β-sheets. f) Crystal structure of the serine-rich repeat protein binding region (SRRP-BR) from the gram-positive bacterium *L. reuteri*, which adopts a β-helix fold.

unit, whose copy number varies between 15 and 46, driving differences in their protein lengths (Fig. 4a). These repeats have conserved periodicity as well as sequence (Fig. 4b, Supplementary Fig. 4). There are 2 interesting features of this 44 aa repeat unit: (1) it contains a heptapeptide "GVVIVTT" that is predicted to be strongly β-aggregation-prone, which explains the large number of regularly spaced β-aggregation motifs in Hil1–Hil4 (Fig. 2b); (2) it is predicted to form 3 β-strands in the same orientation (Fig. 4b), raising an interesting question of whether the tandem repeats may adopt a β-structure similar to that of the effector domain. Hil7 and Hil8 encode the same repeat unit but have only one copy (Fig. 4a, red boxes). By contrast, Hil5 and Hil6 encode very different low-complexity repeats with a unit length of ~5 aa. Their copy numbers range between 15 and 49 (Fig. 4, c and d), and their sequences have relatively low Ser/Thr frequencies (Fig. 2c). Another consequence of encoding only 1 or 0 copies of the 44 aa repeat unit found in Hil1–Hil4 is that Hil5–Hil8 are predicted to have 2–4 β-aggregation–prone sequences in contrast to 21–50 in Hil1–Hil4. For comparison, characterized yeast adhesins contain 1–3 such sequences at a cut-off of >30% β-aggregation potential predicted by TANGO (Fernandez-Escamilla *et al.* 2004; Ramsook *et al.* 2010; Lipke 2018). The variable lengths, Ser/Thr frequencies, and distribution of β-aggregation sequences, all resulting from the evolution of the tandem repeats, suggest the intriguing possibility that the 8 different Hil proteins in *C. auris* are nonredundant, playing distinct roles in cell adhesion and other cell wall–related phenotypes.

Because tandem repeats are prone to recombination-mediated expansions and contractions, we asked if there are variable numbers of tandem repeats (VNTR) among strains in *C. auris*, which could generate diversity in cell adhesive properties as shown in *S. cerevisiae* (Verstrepen *et al.* 2005). To answer this question, we identified homologs of Hil1–Hil4 in 9 *C. auris* strains from 3 geographically stratified clades (Muñoz *et al.* 2018, 2021). The genomes of these strains were de novo–assembled using long-read technologies (Supplementary Table 4), which allowed us to confidently assess copy number variations within tandem repeats. We identified a total of 8 indel polymorphisms in Hil1–Hil4 (Supplementary Table 5, example alignments in Supplementary Fig. 5). Except for 1 16 aa deletion that is in a single Clade III strain, all 7 other indels span 1 or multiples of the repeat unit and affect all strains within a clade. This is consistent with them being driven by recombination between repeats. The agreement within clades additionally shows the indels are not due to sequencing/assembly artifacts, which are not expected to follow the clade labels. As previously reported, Clade II strains lack 5 of the 8 Hil family proteins, including Hil1-4 (Muñoz *et al.* 2021). Our phylogenetic analysis further showed that this was due to gene losses within Clade II (Supplementary Fig. 6). The potential relationship between the Hil family size and the virulence profiles of Clade II strains is discussed later.

Natural selection on the effector domain during the Hil family expansion in *C. auris*

Gene duplication provides raw materials for natural selection and is often followed by a period of relaxed functional constraints on one or both copies, allowing for sub- or neo-functionalization (Zhang 2003; Innan and Kondrashov 2010). Positive selection can be

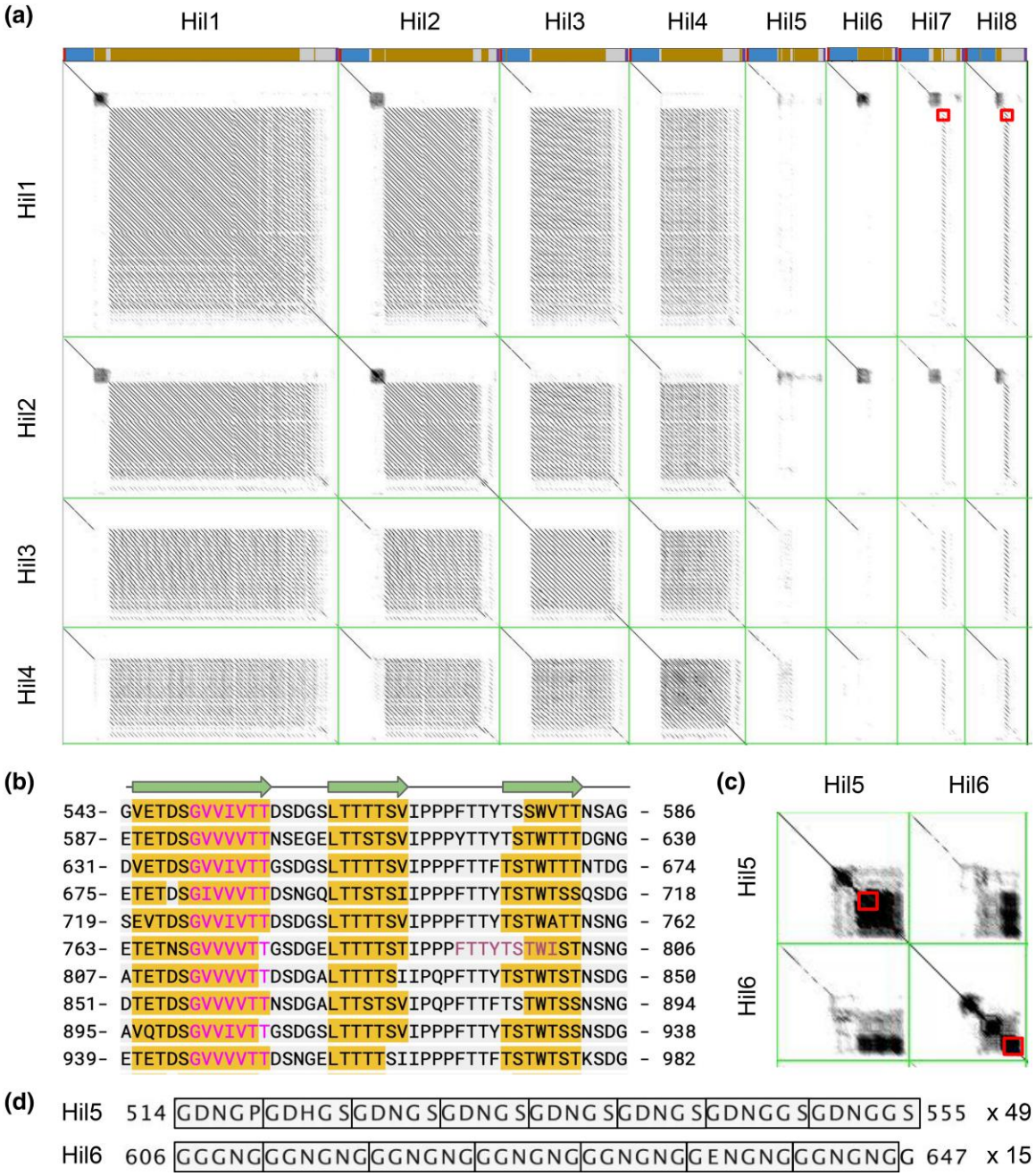

Fig. 4. Dotplot shows the tandem repeat structure within and similarity between *C. auris* Hil proteins. a) Hil1–Hil4 are compared to all 8 Hil proteins in *C. auris* including themselves in dotplots with a sliding window of 50 aa and Grey Map set to 60–245 (min–max). A schematic for each protein is shown above each column (colors same as in Fig. 2). The regions highlighted by the boxes in row 1 reveal the presence of a single copy of the 44 aa repeat unit in Hil7 and Hil8. b) Wrapped sequence of aa 543–982 from Hil1 showing the conserved period and sequence of the 44 aa tandem repeat. Variants of the GVVIVTT motif have strong (probability > 90%) predicted β-aggregation potential while the FTTYTSTWI motif is predicted to have moderate (30–90%) β-aggregation potential. The highlighted regions are predicted by PSIPred to form β-strands, with cartoons shown above. c) Dotplots between Hil5 and Hil6 with the same settings as in (a), showing the low-complexity repeats unique to these two proteins. Regions within the 2 boxes are shown in (d), with residue numbers shown on both ends. The rectangles delineate individual repeats, with the number of copies for each repeat shown to the right.

involved in this process, which can lead to a ratio of nonsynonymous to synonymous substitution rates dN/dS > 1 (Yang 1998). Here, we ask if the Hyphal_reg_CWP domain in *C. auris* Hil1–Hil8 experienced relaxed selective constraints and/or positive selection following gene duplications, the latter of which would suggest functional diversification. We chose to focus on the Hyphal_reg_CWP domain because of its functional importance and because the high-quality alignment in this domain allowed us to make confident evolutionary inferences (Supplementary Fig. 7).

Because gene conversion between paralogs can cause distinct genealogical histories for different parts of the alignment and mislead evolutionary inferences (Casola and Hahn 2009), we first identified putatively nonrecombining partitions using GARD (Kosakovsky Pond *et al.* 2006) (Supplementary Fig. 8) and chose 2 partitions, P1-414 and P697-981, for maximum likelihood–based analyses using PAML (Yang 2007) (Fig. 5a).

We first tested if a subset of the sites evolved under positive selection consistently on *all* branches. We found moderate evidence

supporting the hypothesis for the P697-981 partition, where the M8 vs M7 and M8 vs M8a tests were significant at a 0.01 level, but the more conservative test M2a vs M1a was not (Supplementary Table 6). All 3 tests were insignificant for the P1-414 partition. Next, we tested for elevated dN/dS on selected branches of the tree, sign of relaxed selective constraints, or positive selection. We first estimated the dN/dS for each branch using a free-ratio model and designated those with dN/dS greater than 10 as the "foreground" (Fig. 5, b and c, "FG"). We found strong evidence for the FG branches to have a higher dN/dS than the remainder of the tree (log–likelihood ratio test $P < 0.01$, Fig. 5d). There is no evidence, however, for the dN/dS across the entire domain on the FG branches to be greater than one (Fig. 5d, *a*, row 2). We then tested the more realistic scenario, where a subset of the sites on the FG branches was subject to positive selection. Using the branch-site test 2 as defined in Zhang *et al.* (2005), we found evidence for positive selection on a subset of the sites on the FG branches for both partitions (log–likelihood ratio test $P < 0.01$) and identified residues in both as candidate targets of positive selection with a posterior probability greater than 0.99 (Fig. 5d). We conclude that there is strong evidence for relaxed selective constraint on the Hyphal_reg_CWP domain on some branches following gene duplications; there is also evidence for positive selection acting on a subset of the sites on those branches. However, as the free-ratio model estimates were noisy and the Empirical Bayes method used to identify the residues under selection lacks power (Zhang *et al.* 2005) and can produce false positives (Nozawa *et al.* 2009), the specific branches and residues implicated must be interpreted with caution.

The yeast Hil family has adhesin-like domain architecture with rapidly diverging central domain sequences

We next examined the entire yeast Hil family to reveal the broader patterns of its evolution. We found that the Hil family in general has elevated Ser/Thr content compared with the rest of the proteome (Supplementary Fig. 9). Moreover, the majority of family members encode tandem repeats in the central domain (Fig. 6a) and contain predicted β-aggregation–prone sequences (Fig. 6b). Together, these features further suggest that most yeast Hil family members encode fungal adhesins. While these key features typical of yeast adhesins are conserved, the yeast Hil family exhibits extreme variation in protein length, in tandem repeat content, as well as in β-aggregation potential (Fig. 6, a and b, Supplementary Fig. 10), extending the pattern seen in *C. auris* (Fig. 2). The length of the protein outside of the Hyphal_reg_CWP domain has a mean ± standard deviation of 822.4 ± 785.8 aa and a median of 608.5 aa. This large variation in protein length is almost entirely driven by the tandem repeats (Fig. 6c, linear regression slope = 1.0, $r^2 = 0.83$). A subset of the Hil proteins (vertical bar in Fig. 6, a and b) stand out in that they are both longer than the rest of the family (1,745 vs 770 aa, median protein length) and have an unusually large number of β-aggregation–prone motifs (25 vs 6, median number of TANGO hits per protein). The motifs in this group of proteins are regularly spaced as a result of being part of the tandem repeat unit (median absolute deviation (MAD) of distances between adjacent TANGO hits less than 5 aa, Fig. 6d). The motif "GVVIVTT" and its variants account for 61% of all hits in this subset and is not found in significant number in the rest of the family. Together, these observations combined with previous experimental studies showing a direct impact of adhesin length and β-aggregation potential on function (Verstrepen *et al.* 2005; Lipke *et al.* 2012) lead us to propose that the rapid divergence of the Hil family members following the parallel expansion of the family led to functional diversification in adhesion in pathogenic yeasts and may have contributed to their enhanced virulence.

The yeast Hil family genes are preferentially located near chromosome ends

Several well-characterized yeast adhesin families, including the Flo family in *S. cerevisiae* and the Epa family in *C. glabrata*, are enriched in the subtelomeres (Teunissen and Steensma 1995; De Las Peñas *et al.* 2003; Xu *et al.* 2020, 2021). This region is associated with high rates of single-nucleotide polymorphisms (SNPs), indels, and copy number variations and can undergo ectopic recombination that enables the spread of genes between chromosome ends or their losses (Mefford and Trask 2002; Anderson *et al.* 2015). To determine if the Hil family is also enriched in the subtelomeric region, we compared their chromosomal locations with the background gene density distribution (Fig. 7a) in species with a chromosomal level assembly (Supplementary Table 7). To account for the shared evolutionary history, we selected one species per closely related group such that the Hil family homologs in these species were mostly derived through independent duplications based on our gene tree (Supplementary Fig. 2). The result showed that the Hil family genes are indeed enriched at chromosomal ends (Fig. 7b). A goodness-of-fit test confirmed that the difference between the chromosomal locations of the Hil family and the genome background is highly significant ($P = 1.3 \times 10^{-12}$). As ectopic recombination between subtelomeres has been suggested to underlie the spread of gene families (Anderson *et al.* 2015), we hypothesize that the enrichment of the Hil family toward the chromosome ends is both a cause and consequence of its parallel expansion in different *Candida* lineages.

Discussion

The repeated emergence of human pathogens in the Saccharomycetes class poses serious health threats, as many emerging pathogenic species are resistant or quickly gain resistance to available antifungal drugs (Lamoth *et al.* 2018; Srivastava *et al.* 2018). This raises an evolutionary question: are there shared genomic changes in independently derived *Candida* pathogens, which could be key factors in host adaptation? Yeast adhesin families were among the most enriched gene families in pathogenic lineages relative to the low pathogenic potential relatives (Butler *et al.* 2009). It has been proposed that expansion of adhesin families could be a key step in the emergence of novel yeast pathogens (Gabaldón *et al.* 2016). However, detailed phylogenetic studies supporting this hypothesis are rare (Gabaldón *et al.* 2013), and far less is known about how their sequences diverge and what selective forces are involved during the expansions (Xie *et al.* 2011; Muñoz *et al.* 2021). In this study, we found that the Hyr/Iff-like (Hil) family, defined by the conserved Hyphal_reg_CWP domain, is significantly enriched among distantly related pathogenic clades (Fig. 1, a and b). This resulted from independent expansion of the family in these clades, including among closely related species (Fig. 1, c and d). We also showed that the protein sequences diverged extremely rapidly after duplications, driven mostly by the evolution of the tandem repeats and resulting in large variations in protein length, Ser/Thr content, and β-aggregation potential (Figs. 2b, c, and 6). Our evolutionary analyses revealed evidence of relaxed selective constraint and a potential role of positive selection acting on the Hyphal_reg_CWP domain during the family's expansion in *C. auris* (Fig. 5). We also found the Hil family to be strongly enriched

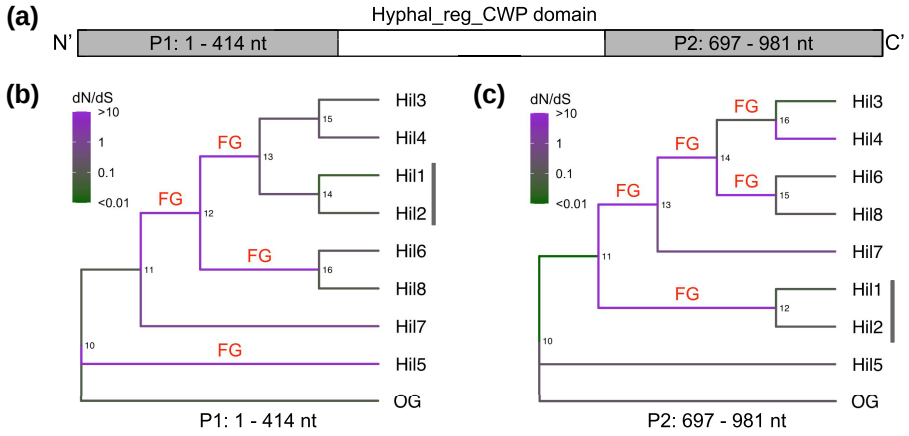

(d)

Tests and models compared	Partition 1-414 nt	Partition 697- 987 nt
a. branch test for variable dN/dS (=ω) between FG=foreground and the rest branches (BG)		
H_0: single dN/dS (ω) H_1: two dN/dS (ω_{FG} free)	$P < 0.001$ $\omega_{FG} = 1.77$, $\omega_{BG} = 0.13$	$P < 0.01$ $\omega_{FG} = 1.53$, $\omega_{BG} = 0.14$
H_0: two dN/dS ($\omega_{FG} == 1$) H_1: two dN/dS (ω_{FG} free)	Insig.	Insig.
b. branch-site test for positive selection		
H_0: no positive selection H_1: positive selection on specific sites in the FG branches	$P < 0.01$ p(ω>1) = 0.53, ω2 = 224.43 *S39, G112*	$P < 0.01$ p(ω>1) = 0.19, ω2 = 9.85 *A234, D287, S304*

Fig. 5. Maximum likelihood–based analyses for selective pressure variation and role of positive selection on the Hyphal_reg_CWP domain in *C. auris*. a) Schematic showing the putative nonrecombining partitions within the Hyphal_reg_CWP domain determined by GARD (see Supplementary Fig. 8). The 2 partitions labeled in gray were studied separately. The numbers refer to the columns in the coding sequence alignment. b, c) Phylogenetic trees were reconstructed for the 2 partitions and are shown as a cladogram. The vertical bar next to the Hil1/Hil2 pair indicates the difference in topology between the 2 trees. Branch colors are based on the dN/dS values estimated from a free-ratio model in PAML. "FG" designate foreground branches, whose dN/dS were greater than 10, except for branch 14..16 in (c), which was selected instead of 16..Hil4 because this would require fewer evolutionary changes in selective forces. We also analyzed the scenario with 16..Hil4 as the foreground, and the conclusions remained the same with slightly different *P*-values. d) Summary of the maximum likelihood–based tests for selective force heterogeneity and for positive selection. "Insig." means *P*-value > 0.05. In the branch-site test, *P*(ω>1) is the total proportion of sites with dN/dS > 1 on the FG branches and ω2 their estimated dN/dS. The listed sites were identified as being under positive selection with a posterior probability greater than 0.99 by the Bayes Empirical Bayes (BEB). The one-letter code and number refer to the amino acid in the OG sequence and the alignment column (Supplementary Fig. 7).

near chromosomal ends (Fig. 7). Overall, our results support the hypothesis that expansion and diversification of adhesin families is a key step toward the emergence of yeast pathogens.

Genome assembly quality limits gene family evolution studies

Like any study of multigene family evolution, our work relies on and is limited by the quality of the genome assemblies. Two additional challenges in our study are due to the fact that Hil family genes are rich in tandem repeats (Figs. 2b and 6a), and many are located near chromosome ends (Fig. 7b), both of which pose problems for genome assemblies. For example, we found significant disagreement in length for 8 of the 16 Hil proteins in *C. tropicalis* between a long-read assembly and the RefSeq assembly, consistent with a recent study (Oh *et al.* 2020) (Supplementary Table 8) and in *C. glabrata*, we identified 13 Hil family genes in a long-read assembly (GCA_010111755.1) vs 3 in the RefSeq assembly (GCF_000002545.3); 12 of the 13 genes were in the subtelomeres (Xu *et al.* 2020). However, similar analyses in additional species did not reveal these problems, suggesting that the issues were at least in part due to difficulties in some genomes (Supplementary Text 1). Nonetheless, we acknowledge the possibility of missing homologs and inaccurate sequences, especially in the tandem repeat region. We thus believe the expected improvements in genome assemblies due to advances in long-read sequencing technologies will be crucial for future studies of the adhesin gene family in yeasts. It is worth noting that our main conclusions about the parallel expansion of the Hil family and its rapid divergence patterns are robust with respect to isolated problems as described above. Also, the long-read technology–based and de novo–assembled genomes for *C. auris* strains allowed us to confidently assess variation in the Hil family size and tandem repeat copy number between paralogs and among individual strains (Supplementary Table 4). The accuracy of the tandem repeat sequences in multiple strains in this species is supported by the conservation of repeat copy numbers within clades (Supplementary Table 5).

Evidence for adhesin functions in the Hil family

A few members of the Hil family, e.g. Iff4 in *C. albicans* and Awp2 in *C. glabrata*, were shown to mediate adhesiveness to polystyrene (Fu *et al.* 2008; Kempf *et al.* 2009; Reithofer *et al.* 2021). While further experimental studies are needed to establish the adhesin functions of other Hil family members, our work provides bioinformatic support for this hypothesis (Figs. 2 and 6). The predicted β-helix fold of the Hyphal_reg_CWP domain (Fig. 3), while unusual among characterized yeast adhesins (Willaert 2018), is

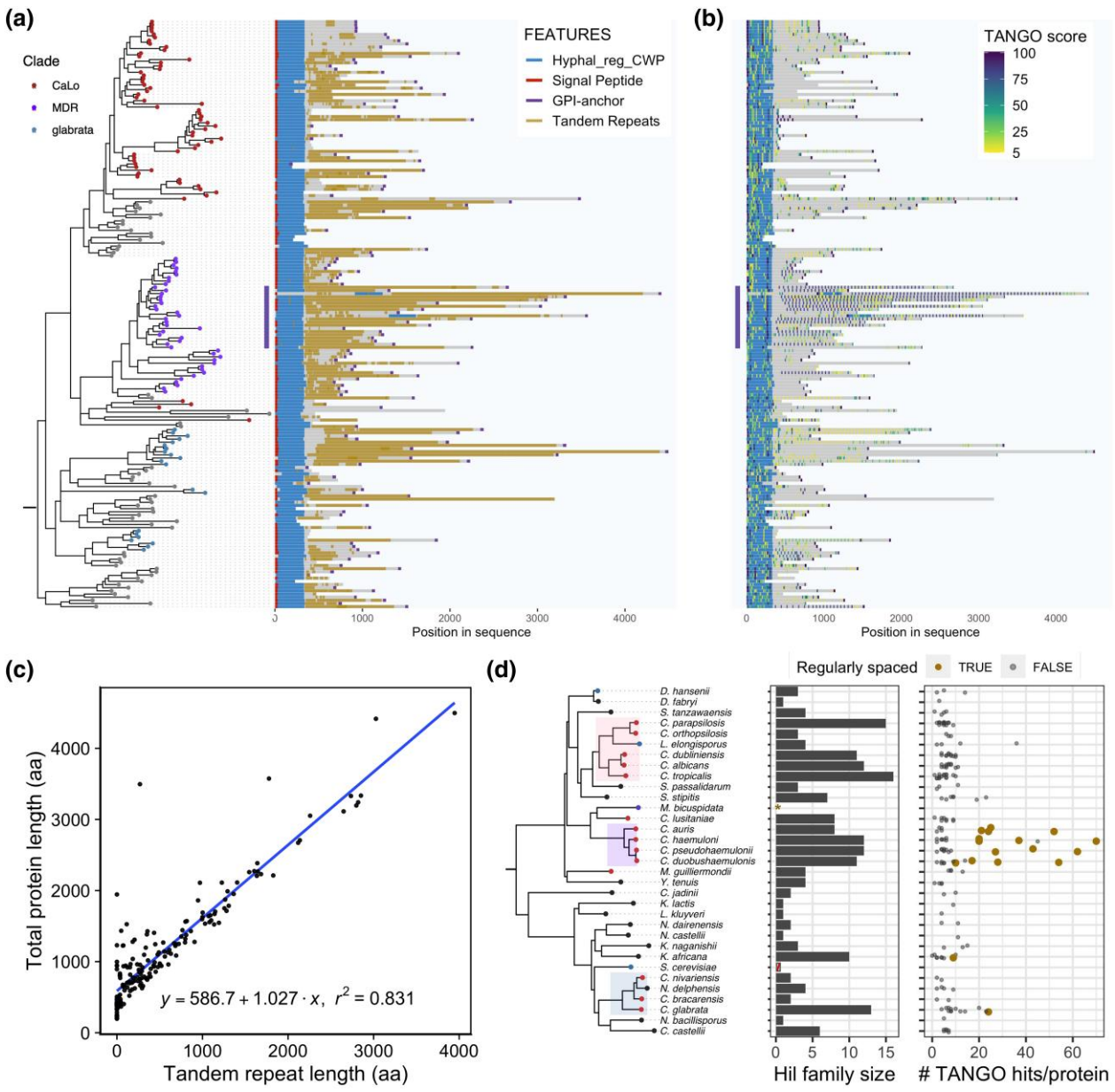

Fig. 6. Evolution of protein length and β-aggregation potential in the yeast Hil family. a) Domain schematic shows that most homologs have a signal peptide at the N-terminus, then the Hyphal_reg_CWP domain, and a highly repetitive region central domain, followed by the C-terminal GPI anchor peptide. Homologs from *M. bicuspidata* were not included because many were annotated as incomplete. They were also excluded from other results in this figure. b) Distribution of TANGO-predicted β-aggregation sequences. The score for each sequence is shown as a color gradient and represents the median of the per-residue probability of aggregation. A vertical bar marks a group of MDR clade sequences that have a large number of β-aggregation–prone sequences arranged in regular intervals. c) X–Y plot showing the relationship between total protein length and tandem repeat sequence length for Hil family homologs. The linear regression line is shown in blue, with coefficients and r^2 values below. d) The species tree on the left is the same as in Fig. 1. The middle panel shows the number of Hil homologs per species. *M. bicuspidata* homologs were excluded; *S. cerevisiae* was included in the species tree, but no Hil homolog was identified in it (see text). The right panel shows the number of predicted β-aggregation–prone motifs per Hil homolog. Only motifs with a median probability ≥30% were counted. Proteins are colored in gold if they have 5 or more such motifs and if the MAD of the inter-motif distances is < 5 aa.

found in many virulence factors residing on the surface of bacteria or viruses as well as enzymes that degrade or modify polysaccharides (Supplementary Table 3) (Kajava and Steven 2006). The elongated shape and rigid structure of the β-helix are consistent with the functional requirements of adhesins, including the need to protrude from the cell surface and the capacity for multiple binding sites along its length that facilitate adhesion. In a bacterial adhesin—the serine-rich repeat protein (SRRP) from the gram-positive bacterium, *L. reuteri*—a protruding, flexible loop in the β-helix was proposed to serve as a binding pocket for its ligand (Sequeira *et al.* 2018). Such a feature is not apparent in the predicted structure of the Hyphal_reg_CWP domain. Further studies are needed to elucidate the mechanism of action of this domain and its potential substrates.

The cross-kingdom similarity in adhesin effector domain structure is intriguing in several ways. First, it suggests convergent evolution in bacteria and yeasts. Second, it suggests that what is known about the structure–function relationship in bacteria can

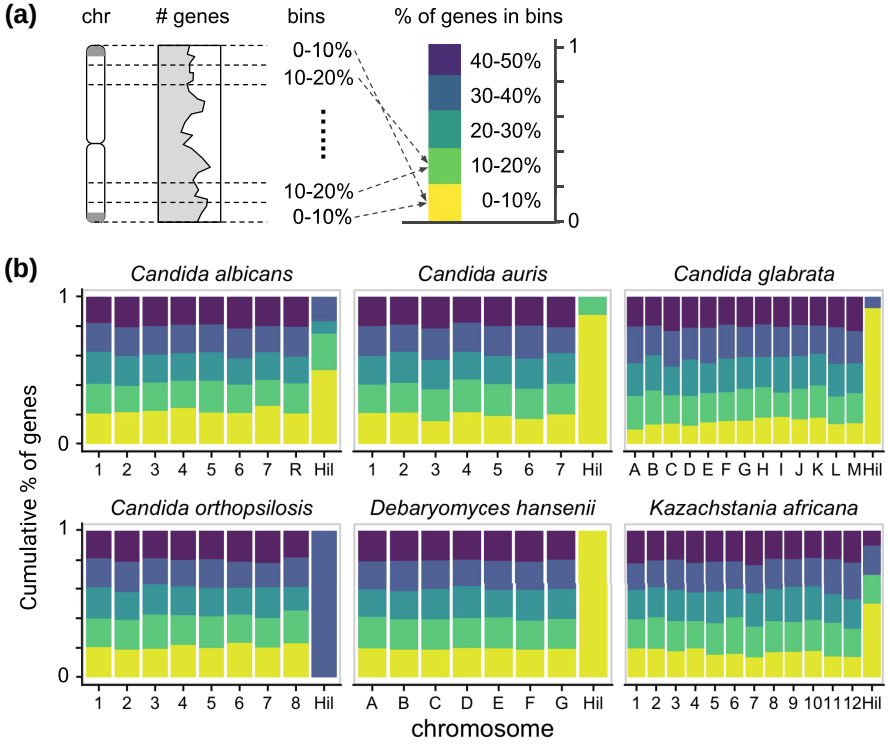

Fig. 7. Hil family genes are preferentially located near the chromosome ends. a) Schematic of the analysis: each chromosome (chr) is folded in half and divided into 5 equal-length "bins," ordered by their distance to the nearest telomere. The cumulative bar graph on the right summarizes the gene density distribution in the 5 bins. b) Folded gene density distribution for 6 species with a chromosomal level assembly and more than 2 Hil family genes. The bin colors are as shown in (a). The Hil homologs in each species are plotted as a separate group. A goodness-of-fit test comparing the distribution of the Hil family genes to the genome background yielded a *P*-value of 1.3×10^{-12}.

provide insight into the Hyphal_reg_CWP domain in yeast. Notably, the *Lr*SRRP shows a pH-dependent substrate specificity that is potentially adapted to distinct host niches (Sequeira *et al.* 2018). Finally, the similar structure and function of the bacterial and yeast adhesins could mediate cross-kingdom interactions in natural and host environments (Uppuluri *et al.* 2018).

However, not all Hil family homologs are likely to encode adhesins. Sequence features suggest some Hil family proteins may have non-adhesin functions. For example, 39 of 193 Hil proteins (homologs labeled as incomplete were excluded) have the requisite signal sequence (SP+) but lack a GPI anchor attachment site (gpi-, Supplementary Fig. 1b). One, Iff11 in *C. albicans*, was shown to be secreted, and a null mutant was found to be hypersensitive to cell wall–damaging agents and less virulent in a murine systemic infection model (Bates *et al.* 2007). Moreover, 75% of these "SP+, gpi-" proteins are shorter than 600 amino acids, in contrast to only 4% of the 117 proteins having both a signal peptide and a GPI anchor attachment site. Such short, secreted proteins with tandem repeat sequences identical or similar to those present in the cell wall–associated Hil protein counterparts may serve an important regulatory function by bundling with wall-associated adhesins as previously suggested for similar subclass of proteins within the Als family (Oh *et al.* 2019). It is possible that the Hil family has evolved diverse functions broadly related to cell adhesion.

Ongoing diversification of the Hil family within species

In addition to the parallel expansion and the subsequent rapid sequence divergence in the Hil family between species, we and others also revealed population-level variation in both the family size and sequences within *C. auris* (Supplementary Figs. 5 and 6, and Supplementary Table 5) (Muñoz *et al.* 2021). Notably, among the 4 geographically stratified clades, Clade II strains lost 5 of the 8 Hil family members (Supplementary Fig. 6). Besides missing members of the Hil family, Clade II strains also lack 7 of the 8 members of another GPI anchor family that is specific to *C. auris* (Muñoz *et al.* 2021). These coincide with the finding that Clade II strains were mostly associated with ear infections (57/61 isolates (Kwon *et al.* 2019)) rather than hospital outbreaks, as reported for strains from the other clades, and that they were generally less resistant to antifungal drugs (Kwon *et al.* 2019; Welsh *et al.* 2019). This raises the question of whether the smaller adhesin repertoire in Clade II strains limits their adhesive capability and results in a different pathology. Similar expansion and contraction of adhesin families have been shown for the *C. glabrata* Hil family (AWP Cluster V) and Epa family (Marcet-Houben *et al.* 2022), suggesting that dynamic evolution of adhesin families in pathogenic yeasts could be a common pattern. Variation in the tandem repeat copy number in Hil1–Hil4 among *C. auris* strains is also intriguing (Supplementary Fig. 5). Prior studies of the *S. cerevisiae* Flo proteins have shown that protein length directly impacts cellular adhesion phenotypes (Verstrepen *et al.* 2005) and thus population-level variation in adhesin length could further contribute to phenotypic diversity. Lastly, scans for selective sweeps in *C. auris* identified Hil and Als family members as being among the top 5% of all genes, suggesting that adhesins are targets of natural selection in the recent evolutionary history of this newly emerged pathogen (Muñoz *et al.* 2021).

Diversification of the adhesin repertoire within a strain can arise from a variety of molecular mechanisms. For example,

chimeric proteins generated through recombination between Als family members or between an Als protein's N-terminal effector domain and an Hyr/Iff protein's repeat region have been shown (Butler *et al.* 2009; Zhao *et al.* 2011; Oh *et al.* 2019). Some of the adhesins with highly diverged central domains may have arisen in this manner (Supplementary Fig. 10). Gene conversion between members of the same family can also drive the evolution of adhesin families within a species, as shown in *S. cerevisiae* and *C. glabrata* (Verstrepen *et al.* 2004; Marcet-Houben *et al.* 2022). Evidence of this in the Hil family was revealed in our analysis of recombination within the effector domain in *C. auris* (Supplementary Fig. 8).

Special properties of the central domain in *C. auris* Hil1–Hil4 and related Hil proteins

A subset of Hil proteins represented by *C. auris* Hil1–Hil4 (Fig. 6, a and b, vertical bar) stands out in that they are much longer on average and encode a large number of β-aggregation–prone sequences compared with the rest of the family (Fig. 6, b and d). Behind these properties is a conserved ∼44 aa repeat unit containing a highly β-aggregation–prone sequence ("GVVIVTT" and its variants) (Fig. 4b). β-aggregation–prone sequences and the amyloid-like interaction they mediate have been extensively studied, especially in the Als protein family in *C. albicans*: they were experimentally shown to mediate aggregation (Otoo *et al.* 2008; Ramsook *et al.* 2010) and were crucial for forming protein clusters on cell surfaces known as nanodomains in response to physical tension or sheer forces (Alsteens *et al.* 2010; Lipke *et al.* 2012). Recently, they were also shown to mediate cell–cell *trans* interactions via homotypic protein binding (Dehullu *et al.* 2019; Ho *et al.* 2019). This may underlie biofilm formation and kin discrimination (Smukalla *et al.* 2008; Brückner *et al.* 2020; Lipke *et al.* 2021). Most known yeast adhesins, including the Als family proteins, encode between 1 and 3 β-aggregation–prone sequences (Ramsook *et al.* 2010). *C. auris* Hil1–Hil4 and their close relatives are unusual in that they have as many as 50 such sequences, with each predicted by TANGO to have ∼90% probability of aggregation, whereas the positive threshold for the algorithm is only >5% over 5–6 residues (Fernandez-Escamilla *et al.* 2004). The structural implications of the vast number of β-aggregation–prone motifs may be that such tandem repeat domains are constitutively amyloid in nature, rather than requiring force or other stimuli as required by the Als proteins. The functional implications are unclear without the requisite experimental tests. However, we speculate that variations in protein length and β-aggregation potential resulting from the central domain divergence could directly impact the adhesion functions as previously suggested (Verstrepen *et al.* 2005; Boisramé *et al.* 2011; Lipke *et al.* 2012).

Structural predictions of the tandem repeat region in *C. auris* Hil1 and Hil2

Given the large number of ∼44 aa repeats in the central domain of *C. auris* Hil1–Hil4 and the prediction that each repeat encodes 3–4 short consecutive β-strands (Fig. 4b), we wondered what structural properties this region may have and how these features might contribute to the adhesion function. We explored this question using threading-based structural prediction tools such as I-TASSER (Yang *et al.* 2015) and pDOMThreader (Lobley *et al.* 2009). For the tandem repeat region in the central domain of Hil1, I-TASSER identified (S)-layer protein (SLP) structures (e.g. RsaA from *Caulobacter crescentus* and SbsA and SbsC from *Geobacillus stearothermophilus*) as among the top structural analogs. These β-strand–rich structures are known to self-assemble to form a 2-dimensional array on the surface of bacteria, mediating a range of functions including adhesion to host cells in pathogens (Fagan and Fairweather 2014). pDOMThreader analyses of the central domains in Hil1 and Hil2 identified a different set of templates, namely, bacterial self-associating proteins including Ag43a from uropathogenic *E. coli*, pertactin from *B. pertussis*, and the *H. influenzae* Hap adhesin. Interestingly, these proteins have β-helical structures like the Hyphal_reg_CWP domain, with the β-helices being involved in cell–cell interaction via an interface along the long solenoidal axis for homotypic interactions, mediate bacterial clumping (Heras *et al.* 2014), and lead to biofilm formation in *H. influenzae* (Meng *et al.* 2011). We speculate that the long repeat regions in Hil1 and Hil2 may similarly mediate cell–cell interactions in *C. auris*.

The possibility that the central domains in Hil1 and Hil2 form a β-helix is interesting in that β-helix is one of the commonly described structural motifs in functional amyloids, e.g. HET-s from the fungus *Podospora anserina* (Wasmer *et al.* 2008). Such a solenoid-type amyloid is distinguished from other amyloid types in that the β-helices formed by repeats within the same protein, rather than among distinct monomeric proteins, are suggested to be stabilized not only by polar zippers and hydrophobic contacts but also by electrostatic interactions between the alternating β-strands (Willbold *et al.* 2021). Other examples of amyloid-forming proteins with a predicted β-helix structure include the imperfect repeat domain in the human premelanosome protein Pmel17 (Louros *et al.* 2016) and the extracellular curli proteins of Enterobacteriaceae that are involved in biofilm formation and adhesion to host cells (Shewmaker et al. 2009). The proposed solenoidal structure of the central domain of Hil1–Hil4 like proteins, if true, would have 2 significant implications. First, it confers the necessary rigidity and extended conformation required for cell wall–anchored adhesins to extend into the surrounding extracellular milieu. Second, the numerous β-strand–rich repeats each containing a highly amyloid-prone heptameric sequence and capable of wrapping into a solenoidal shaped stack are likely to substantially reduce the rate-limiting nucleation step, which limits the formation of, e.g., an Aβ amyloid fiber. This would allow the formation of extracellular extensions at low protein concentrations without the need for an extensive fiber-lengthening process via the incorporation of additional monomeric units. Finally, the observation of solenoid-mediated intercellular interactions in the Hap adhesins suggests that Hil proteins may likewise have a biofilm-related function.

Genomic context

As reported by Muñoz *et al.* (2021), we found that the Hil family genes are preferentially located near chromosomal ends in *C. auris* and also in other species examined (Fig. 7). This is similar to previous findings for the Flo and Epa families (Teunissen and Steensma 1995; De Las Peñas *et al.* 2003; Xu *et al.* 2020, 2021), as well as the Als genes in some species (Oh *et al.* 2021). This location bias of the Hil and other adhesin families is likely a key mechanism for their dynamic expansion and sequence evolution via ectopic recombination (Anderson *et al.* 2015) and by break-induced replication (Bosco and Haber 1998; Sakofsky and Malkova 2017; Xu *et al.* 2021). Another potential consequence of the Hil family genes being located in subtelomeres is that they may be subject to epigenetic silencing as an additional regulatory mechanism, which can be derepressed in response to stress (Ai *et al.* 2002). Such epigenetic regulation of the adhesin genes was found to generate cell surface heterogeneity in *S. cerevisiae* (Halme *et al.* 2004) and leads to hyperadherent phenotypes in *C. glabrata* (Castaño *et al.* 2005).

Conclusion

To address the lack of candidate adhesins in *C. auris*, we identified and characterized the Hil family in this species and all yeasts. Based on our results, we hypothesize that expansion and diversification of adhesin gene families is a key step toward the evolution of fungal pathogenesis and that variation in the adhesin repertoire contributes to within- and between-species differences in the adhesive and virulence properties. Future experimental tests of these hypotheses will be important biologically for improving our understanding of the fungal adhesin repertoire, biotechnologically for inspiring additional nanomaterials, and biomedically for advancing the development of *C. auris*–directed therapeutics.

Data availability

Raw data and analysis scripts are available at https://doi.org/10.5281/zenodo.7631150. The version and reference of the main analysis software are listed in Table 1.

Supplemental material available at GENETICS online.

Acknowledgments

This study was inspired by work conducted during a bioinformatics course (BIOL:4213) in Fall of 2019, whose semester theme was the recently published *C. auris* genomes. Graduate students, LS and RS, were lead investigators on a group project centered on the genes containing the Hyphal_reg_CWP (PF11765) domain during that course and were happy to be invited to continue working on these genes long after the semester ended. We would also like to thank members of the Gene Regulatory Evolution lab for discussion. We thank Drs. Yong Zhang (CAS Zoology Institute), Peter Lipke (Brooklyn College), John McCutcheon (ASU), Matthew Anderson (OSU), Matthew Hahn (Indiana University), Rich Lenski (MSU), Josep Comeron (University of Iowa), Daniel Weeks (University of Iowa), Lois Hoyer (UIUC) and 2 other anonymous reviewers for providing useful suggestions and critical comments.

Funding

BZH is supported by NIH R35GM137831. JSF is supported by NSF-IOS-1917169. LFS was supported by the NIH Predoctoral Training grant T32GM008629. RAS is supported by an NSF Graduate Research Fellowship Program under Grant No. 1546595, with additional support through the NSF Division of Graduate Education under Grant No. 1633098.

Conflicts of interest

The authors declare no conflict of interest.

Literature cited

Ai W, Bertram PG, Tsang CK, Chan TF, Zheng XFS. Regulation of subtelomeric silencing during stress response. Mol Cell. 2002;10(6):1295–1305. doi:10.1016/S1097-2765(02)00695-0

Alsteens D, Garcia MC, Lipke PN, Dufrêne YF. Force-induced formation and propagation of adhesion nanodomains in living fungal cells. Proc Natl Acad Sci USA. 2010;107(48):20744–20749. doi:10.1073/pnas.1013893107

Anderson MZ, Wigen LJ, Burrack LS, Berman J. Real-time evolution of a subtelomeric gene family in *Candida albicans*. Genetics. 2015;200(3):907–919. doi:10.1534/genetics.115.177451

Bailey DA, Feldmann PJ, Bovey M, Gow NA, Brown AJ. The Candida albicans HYR1 gene, which is activated in response to hyphal development, belongs to a gene family encoding yeast cell wall proteins. J Bacteriol. 1996;178(18):5353–5360. doi:10.1128/jb.178.18.5353-5360.1996

Bates S, de la Rosa JM, MacCallum DM, Brown AJP, Gow NAR, Odds FC. *Candida albicans* Iff11, a secreted protein required for cell wall structure and virulence. Infect Immun. 2007;75(6):2922–2928. doi:10.1128/IAI.00102-07

Berger SA, Krompass D, Stamatakis A. Performance, accuracy, and web server for evolutionary placement of short sequence reads under maximum likelihood. Syst Biol. 2011;60(3):291–302. doi:10.1093/sysbio/syr010

Boisramé A, Cornu A, Da Costa G, Richard ML. Unexpected role for a serine/threonine-rich domain in the Candida albicans iff protein family. Eukaryot Cell. 2011;10(10):1317–1330. doi:10.1128/EC.05044-11

Bosco G, Haber JE. Chromosome break-induced DNA replication leads to nonreciprocal translocations and telomere capture. Genetics. 1998;150(3):1037–1047. doi:10.1093/genetics/150.3.1037

Bradley PH, Nayfach S, Pollard KS. Phylogeny-corrected identification of microbial gene families relevant to human gut colonization. PLoS Comput Biol. 2018;14(8):e1006242. doi:10.1371/journal.pcbi.1006242

Brodie R, Roper RL, Upton C. JDotter: a Java interface to multiple dotplots generated by dotter. Bioinformatics. 2004;20(2):279–281. doi:10.1093/bioinformatics/btg406

Brückner S, Schubert R, Kraushaar T, Hartmann R, Hoffmann D, Jelli E, Drescher K, Müller DJ, Oliver Essen L, Mösch H-U. Kin discrimination in social yeast is mediated by cell surface receptors of the Flo11 adhesin family. eLife. 2020;9:e55587. doi:10.7554/eLife.55587

Buchan DWA, Jones DT. The PSIPRED protein analysis workbench: 20 years on. Nucleic Acids Res. 2019;47(W1):W402–W407. doi:10.1093/nar/gkz297

Butler G, Rasmussen MD, Lin MF, Santos MAS, Sakthikumar S, Munro CA, Rheinbay E, Grabherr M, Forche A, Reedy JL, *et al.* Evolution of pathogenicity and sexual reproduction in eight Candida genomes. Nature. 2009;459(7247):657–662. doi:10.1038/nature08064

Camacho C, Coulouris G, Avagyan V, Ma N, Papadopoulos J, Bealer K, Madden TL. BLAST+: architecture and applications. BMC Bioinformatics. 2009;10(1):421. doi:10.1186/1471-2105-10-421

Casola C, Hahn MW. Gene conversion among paralogs results in moderate false detection of positive selection using likelihood methods. J Mol Evol. 2009;68(6):679–687. doi:10.1007/s00239-009-9241-6

Castaño I, Pan S-J, Zupancic M, Hennequin C, Dujon B, Cormack BP. Telomere length control and transcriptional regulation of subtelomeric adhesins in Candida glabrata. Mol Microbiol. 2005;55(4):1246–1258. doi:10.1111/j.1365-2958.2004.04465.x

CDC. 2019 Antibiotic resistance threats in the United States, 2019. US Dep. Health Hum. Serv. CDC. http://dx.doi.org/10.15620/cdc:82532.

Chaudhuri R, Ansari FA, Raghunandanan MV, Ramachandran S. FungalRV: adhesin prediction and immunoinformatics portal for human fungal pathogens. BMC Genomics. 2011;12(1):192. doi:10.1186/1471-2164-12-192

de Groot PWJ, Bader O, de Boer AD, Weig M, Chauhan N. Adhesins in human fungal pathogens: glue with plenty of stick. Eukaryot Cell. 2013;12(4):470–481. doi:10.1128/EC.00364-12

Dehullu J, Valotteau C, Herman-Bausier P, Garcia-Sherman M, Mittelviefhaus M, Vorholt JA, Lipke PN, Dufrêne YF. Fluidic force microscopy demonstrates that homophilic adhesion by *Candida*

albicans als proteins is mediated by amyloid bonds between cells. Nano Lett. 2019;19(6):3846–3853. doi:10.1021/acs.nanolett.9b01010

De Las Peñas A, Pan S-J, Castaño I, Alder J, Cregg R, Cormack BP. Virulence-related surface glycoproteins in the yeast pathogen *Candida glabrata* are encoded in subtelomeric clusters and subject to *RAP1*- and *SIR*-dependent transcriptional silencing. Genes Dev. 2003;17(18):2245–2258. doi:10.1101/gad.1121003

Dujon B, Sherman D, Fischer G, Durrens P, Casaregola S, Lafontaine I, de Montigny J, Marck C, Neuvéglise C, Talla E, *et al.* Genome evolution in yeasts. Nature. 2004;430(6995):35–44. doi:10.1038/nature02579

Eberlein C, Nielly-Thibault L, Maaroufi H, Dubé AK, Leducq J-B, Charron G, Landry CR. The rapid evolution of an ohnolog contributes to the ecological specialization of incipient yeast species. Mol Biol Evol. 2017;34(9):2173–2186. doi:10.1093/molbev/msx153

Engels B. XNomial: exact goodness-of-fit test for multinomial data with fixed probabilities. Vienna (Austria): CRAN; 2015.

Fagan RP, Fairweather NF. Biogenesis and functions of bacterial S-layers. Nat Rev Microbiol. 2014;12(3):211–222. doi:10.1038/nrmicro3213

Fernandez-Escamilla A-M, Rousseau F, Schymkowitz J, Serrano L. Prediction of sequence-dependent and mutational effects on the aggregation of peptides and proteins. Nat Biotechnol. 2004;22(10):1302–1306. doi:10.1038/nbt1012

Frank AT, Ramsook CB, Otoo HN, Tan C, Soybelman G, Rauceo JM, Gaur NK, Klotz SA, Lipke PN. Structure and function of glycosylated tandem repeats from Candida albicans als adhesins. Eukaryot Cell. 2010;9(3):405–414. doi:10.1128/EC.00235-09

Frieman MB, McCaffery JM, Cormack BP. Modular domain structure in the *Candida glabrata* adhesin Epa1p, a beta1,6 glucan-cross-linked cell wall protein. Mol Microbiol. 2002;46(2):479–492. doi:10.1046/j.1365-2958.2002.03166.x

Fu Y, Luo G, Spellberg BJ, Edwards JE, Ibrahim AS. Gene overexpression/suppression analysis of candidate virulence factors of *Candida albicans*. Eukaryot Cell. 2008;7(3):483–492. doi:10.1128/EC.00445-07

Gabaldón T, Martin T, Marcet-Houben M, Durrens P, Bolotin-Fukuhara M, Lespinet O, Arnaise S, Boisnard S, Aguileta G, Atanasova R, *et al.* Comparative genomics of emerging pathogens in the Candida glabrata clade. BMC Genomics. 2013;14(1):623. doi:10.1186/1471-2164-14-623

Gabaldón T, Naranjo-Ortíz MA, Marcet-Houben M. Evolutionary genomics of yeast pathogens in the saccharomycotina. FEMS Yeast Res. 2016;16(6):fow064. doi:10.1093/femsyr/fow064

Gordon JL, Armisén D, Proux-Wéra E, ÓhÉigeartaigh SS, Byrne KP, Wolfe KH. Evolutionary erosion of yeast sex chromosomes by mating-type switching accidents. Proc Natl Acad Sci USA. 2011;108(50):20024–20029. doi:10.1073/pnas.1112808108

Gupta R, Brunak S. Prediction of glycosylation across the human proteome and the correlation to protein function. Pac Symp Biocomput. 2002:310–322.

Hall SR, Becker CR, Duffy MA, Cáceres CE. Variation in resource acquisition and use among host clones creates key epidemiological trade-offs. Am Nat. 2010;176(5):557–565. doi:10.1086/656523

Halme A, Bumgarner S, Styles C, Fink GR. Genetic and epigenetic regulation of the FLO gene family generates cell-surface variation in yeast. Cell. 2004;116(3):405–415. doi:10.1016/S0092-8674(04)00118-7

Heras B, Totsika M, Peters KM, Paxman JJ, Gee CL, Jarrott RJ, Perugini MA, Whitten AE, Schembri MA. The antigen 43 structure reveals a molecular Velcro-like mechanism of autotransporter-mediated bacterial clumping. Proc Natl Acad Sci USA. 2014;111(1):457–462. doi:10.1073/pnas.1311592111

Ho V, Herman-Bausier P, Shaw C, Conrad KA, Garcia-Sherman MC, Draghi J, Dufrene YF, Lipke PN, Rauceo JM. An amyloid core sequence in the major Candida albicans adhesin Als1p mediates cell-cell adhesion. mBio. 2019;10(5):e01766–19. doi:10.1128/mBio.01766-19

Ho L, Si T, Ané C. A linear-time algorithm for Gaussian and non-Gaussian trait evolution models. Syst Biol. 2014;63(3):397–408. doi:10.1093/sysbio/syu005

Holm L. Dali server: structural unification of protein families. Nucleic Acids Res. 2022;50(W1):W210. doi:10.1093/nar/gkac387

Hoyer LL. The ALS gene family of Candida albicans. Trends Microbiol. 2001;9(4):176–180. doi:10.1016/S0966-842X(01)01984-9

Hoyer LL, Green CB, Oh S-H, Zhao X. Discovering the secrets of the *Candida albicans* agglutinin-like sequence (ALS) gene family–a sticky pursuit. Med Mycol. 2008;46(1):1–15. doi:10.1080/13693780701435317

Innan H, Kondrashov F. The evolution of gene duplications: classifying and distinguishing between models. Nat Rev Genet. 2010;11(2):97–108. doi:10.1038/nrg2689

Ives AR, Garland T. Phylogenetic logistic regression for binary dependent variables. Syst Biol. 2010;59(1):9–26. doi:10.1093/sysbio/syp074

Jenull S, Tscherner M, Kashko N, Shivarathri R, Stoiber A, Chauhan M, Petryshyn A, Chauhan N, Kuchler K. Transcriptome signatures predict phenotypic variations of Candida auris. Front Cell Infect Microbiol. 2021;11. doi:10.3389/fcimb.2021.662563

Jiang H, Bao J, Xing Y, Li X, Chen Q. Comparative genomic analyses provide insight into the pathogenicity of metschnikowia bicuspidata LNES0119. Front Microbiol. 2022;13:939141. doi:10.3389/fmicb.2022.939141

Jumper J, Evans R, Pritzel A, Green T, Figurnov M, Ronneberger O, Tunyasuvunakool K, Bates R, Žídek A, Potapenko A, *et al.* Highly accurate protein structure prediction with AlphaFold. Nature. 2021;596(7873):583–589. doi:10.1038/s41586-021-03819-2

Kajava AV, Steven AC. The turn of the screw: variations of the abundant beta-solenoid motif in passenger domains of type V secretory proteins. J Struct Biol. 2006;155(2):306–315. doi:10.1016/j.jsb.2006.01.015

Kean R, Delaney C, Sherry L, Borman A, Johnson EM, Richardson MD, Rautemaa-Richardson R, Williams C, Ramage G. Transcriptome assembly and profiling of *Candida auris* reveals novel insights into biofilm-mediated resistance. mSphere. 2018;3(4). doi:10.1128/mSphere.00334-18

Kempf M, Cottin J, Licznar P, Lefrançois C, Robert R, Apaire-Marchais V. Disruption of the GPI protein-encoding gene IFF4 of Candida albicans results in decreased adherence and virulence. Mycopathologia. 2009;168(2):73–77. doi:10.1007/s11046-009-9201-0

Kosakovsky Pond SL, Posada D, Gravenor MB, Woelk CH, Frost SDW. Automated phylogenetic detection of recombination using a genetic algorithm. Mol Biol Evol. 2006;23(10):1891–1901. doi:10.1093/molbev/msl051

Koteiche HA, Mchaourab HS. Folding pattern of the alpha-crystallin domain in alphaA-crystallin determined by site-directed spin labeling. J Mol Biol. 1999;294(2):561–577. doi:10.1006/jmbi.1999.3242

Kozlov AM, Darriba D, Flouri T, Morel B, Stamatakis A. RAxML-NG: a fast, scalable and user-friendly tool for maximum likelihood phylogenetic inference. Bioinformatics. 2019;35(21):4453–4455. doi:10.1093/bioinformatics/btz305

Kuang MC, Hutchins PD, Russell JD, Coon JJ, Hittinger CT. Ongoing resolution of duplicate gene functions shapes the diversification of a metabolic network. eLife. 2016;5:e19027. doi:10.7554/eLife.19027

Kwon YJ, Shin JH, Byun SA, Choi MJ, Won EJ, Lee D, Lee SY, Chun S, Lee JH, Choi HJ, *et al.* Candida auris clinical isolates from South Korea: identification, antifungal susceptibility, and genotyping. J Clin Microbiol. 2019;57(4):e01624–18. doi:10.1128/JCM.01624-18

Lamoth F, Lockhart SR, Berkow EL, Calandra T. Changes in the epidemiological landscape of invasive candidiasis. J Antimicrob Chemother. 2018;73(suppl_1):i4–i13. doi:10.1093/jac/dkx444

Levy A, Salas Gonzalez I, Mittelviefhaus M, Clingenpeel S, Herrera Paredes S, Miao J, Wang K, Devescovi G, Stillman K, Monteiro F, *et al.* Genomic features of bacterial adaptation to plants. Nat Genet. 2018;50(1):138–150. doi:10.1038/s41588-017-0012-9

Linder T, Gustafsson CM. Molecular phylogenetics of ascomycotal adhesins—a novel family of putative cell-surface adhesive proteins in fission yeasts. Fungal Genet Biol. 2008;45(4):485–497. doi:10.1016/j.fgb.2007.08.002

Lipke PN. What we do not know about fungal cell adhesion molecules. J Fungi. 2018;4(2):59. doi:10.3390/jof4020059

Lipke PN, Garcia MC, Alsteens D, Ramsook CB, Klotz SA, Dufrêne YF. Strengthening relationships: amyloids create adhesion nanodomains in yeasts. Trends Microbiol. 2012;20(2):59–65. doi:10.1016/j.tim.2011.10.002

Lipke PN, Mathelié-Guinlet M, Viljoen A, Dufrêne YF. A new function for amyloid-like interactions: cross-beta aggregates of adhesins form cell-to-cell bonds. Pathogens. 2021;10(8):1013. doi:10.3390/pathogens10081013

Lobley A, Sadowski MI, Jones DT. pGenTHREADER and pDomTHREADER: new methods for improved protein fold recognition and superfamily discrimination. Bioinformatics. 2009;25(14):1761–1767. doi:10.1093/bioinformatics/btp302

Lockhart SR, Etienne KA, Vallabhaneni S, Farooqi J, Chowdhary A, Govender NP, Colombo AL, Calvo B, Cuomo CA, Desjardins CA, *et al.* Simultaneous emergence of multidrug-resistant *Candida auris* on 3 continents confirmed by whole-genome sequencing and epidemiological analyses. Clin Infect Dis. 2017;64(2):134–140. doi:10.1093/cid/ciw691

Louros NN, Baltoumas FA, Hamodrakas SJ, Iconomidou VA. A β-solenoid model of the Pmel17 repeat domain: insights to the formation of functional amyloid fibrils. J Comput Aided Mol Des. 2016;30(2):153–164. doi:10.1007/s10822-015-9892-x

Luo G, Ibrahim A, Spellberg B, Nobile C, Mitchell A, Fu Y. *Candida albicans* Hyr1p confers resistance to neutrophil killing and is a potential vaccine target. J Infect Dis. 2010;201(11):1718–1728. doi:10.1086/652407

Marcet-Houben M, Alvarado M, Ksiezopolska E, Saus E, de Groot PWJ, Gabaldón T. Chromosome-level assemblies from diverse clades reveal limited structural and gene content variation in the genome of Candida glabrata. BMC Biol. 2022;20(1):226. doi:10.1186/s12915-022-01412-1

Mefford HC, Trask BJ. The complex structure and dynamic evolution of human subtelomeres. Nat Rev Genet. 2002;3(2):91–102. doi:10.1038/nrg727

Meng G, Spahich N, Kenjale R, Waksman G, St Geme JW. Crystal structure of the *Haemophilus influenzae* hap adhesin reveals an intercellular oligomerization mechanism for bacterial aggregation. EMBO J. 2011;30(18):3864–3874. doi:10.1038/emboj.2011.279

Morel B, Kozlov AM, Stamatakis A, Szöllősi GJ. GeneRax: a tool for species-tree-aware maximum likelihood-based gene family tree inference under gene duplication, transfer, and loss. Mol Biol Evol. 2020;37(9):2763–2774. doi:10.1093/molbev/msaa141

Muñoz JF, Gade L, Chow NA, Loparev VN, Juieng P, Berkow EL, Farrer RA, Litvintseva AP, Cuomo CA. Genomic insights into multidrug-resistance, mating and virulence in Candida auris and related emerging species. Nat Commun. 2018;9(1):5346. doi:10.1038/s41467-018-07779-6

Muñoz JF, Welsh RM, Shea T, Batra D, Gade L, Howard D, Rowe LA, Meis JF, Litvintseva AP, Cuomo CA. Clade-specific chromosomal rearrangements and loss of subtelomeric adhesins in *Candida auris*. Genetics. 2021;218(1). doi:10.1093/genetics/iyab029

Newman AM, Cooper JB. XSTREAM: a practical algorithm for identification and architecture modeling of tandem repeats in protein sequences. BMC Bioinformatics. 2007;8(1):382. doi:10.1186/1471-2105-8-382

Nozawa M, Suzuki Y, Nei M. Reliabilities of identifying positive selection by the branch-site and the site-prediction methods. Proc Natl Acad Sci. 2009;106(16):6700–6705. doi:10.1073/pnas.0901855106

Oh S-H, Isenhower A, Rodriguez-Bobadilla R, Smith B, Jones J, Hubka V, Fields C, Hernandez A, Hoyer LL. Pursuing advances in DNA sequencing technology to solve a complex genomic jigsaw puzzle: the agglutinin-like sequence (ALS) genes of Candida tropicalis. Front Microbiol. 2020;11:594531. doi:10.3389/fmicb.2020.594531

Oh S-H, Schliep K, Isenhower A, Rodriguez-Bobadilla R, Vuong VM, Fields CJ, Hernandez AG, Hoyer LL. Using genomics to shape the definition of the agglutinin-like sequence (ALS) family in the saccharomycetales. Front Cell Infect Microbiol. 2021;11:794529. doi:10.3389/fcimb.2021.794529

Oh S-H, Smith B, Miller AN, Staker B, Fields C, Hernandez A, Hoyer LL. Agglutinin-like sequence (ALS) genes in the Candida parapsilosis species complex: blurring the boundaries between gene families that encode cell-wall proteins. Front Microbiol. 2019;10:781. doi:10.3389/fmicb.2019.00781

Otoo HN, Lee KG, Qiu W, Lipke PN. *Candida albicans* als adhesins have conserved amyloid-forming sequences. Eukaryot Cell. 2008;7(5):776–782. doi:10.1128/EC.00309-07

Pierleoni A, Martelli PL, Casadio R. PredGPI: a GPI-anchor predictor. BMC Bioinformatics. 2008;9(1):392. doi:10.1186/1471-2105-9-392

Potter SC, Luciani A, Eddy SR, Park Y, Lopez R, Finn RD. HMMER web server: 2018 update. Nucleic Acids Res. 2018;46(W1):W200–W204. doi:10.1093/nar/gky448

Qian W, Zhang JG. Genomic evidence for adaptation by gene duplication. Genome Res. 2014;24(8):1356–1362. 10.1101/gr.172098.114

Ramsook CB, Tan C, Garcia MC, Fung R, Soybelman G, Henry R, Litewka A, O'Meally S, Otoo HN, Khalaf RA, *et al.* Yeast cell adhesion molecules have functional amyloid-forming sequences. Eukaryot Cell. 2010;9(3):393–404. doi:10.1128/EC.00068-09

Rauceo JM, De Armond R, Otoo H, Kahn PC, Klotz SA, Gaur NK, Lipke PN. Threonine-rich repeats increase fibronectin binding in the *Candida albicans* adhesin Als5p. Eukaryot Cell. 2006;5(10):1664–1673. doi:10.1128/EC.00120-06

R Core Team. R: a language and environment for statistical computing. Vienna (Austria): R Foundation for Statistical Computing; 2021.

Reid SD, Herbelin CJ, Bumbaugh AC, Selander RK, Whittam TS. Parallel evolution of virulence in pathogenic Escherichia coli. Nature. 2000;406(6791):64–67. doi:10.1038/35017546

Reithofer V, Fernández-Pereira J, Alvarado M, de Groot P, Essen L-O. A novel class of Candida glabrata cell wall proteins with β-helix fold mediates adhesion in clinical isolates. PLoS Pathog. 2021;17(12):e1009980. doi:10.1371/journal.ppat.1009980

Rice P, Longden I, Bleasby A. EMBOSS: the European Molecular Biology Open Software Suite. Trends Genet. 2000;16(6):276–277. doi:10.1016/S0168-9525(00)02024-2

Richard ML, Plaine A. Comprehensive analysis of glycosylphosphatidylinositol-anchored proteins in *Candida albicans*. Eukaryot Cell. 2007;6(2):119–133. doi:10.1128/EC.00297-06

Rosiana S, Zhang L, Kim GH, Revtovich AV, Uthayakumar D, Sukumaran A, Geddes-McAlister J, Kirienko NV, Shapiro RS.

Comprehensive genetic analysis of adhesin proteins and their role in virulence of *Candida albicans*. Genetics. 2021;217(2). doi:10.1093/genetics/iyab003

RStudio Team. RStudio: integrated development environment for R. Boston (MA): RStudio, PBC; 2021.

Sakofsky CJ, Malkova A. Break induced replication in eukaryotes: mechanisms, functions, and consequences. Crit Rev Biochem Mol Biol. 2017;52(4):395–413. doi:10.1080/10409238.2017.1314444

Schrödinger LLC. The PyMOL Molecular Graphics System, Version 2.5.2. New York: Schrödinger LLC; 2021.

Sequeira S, Kavanaugh D, MacKenzie DA, Šuligoj T, Walpole S, Leclaire C, Gunning AP, Latousakis D, Willats WGT, Angulo J, *et al.* Structural basis for the role of serine-rich repeat proteins from *Lactobacillus reuteri* in gut microbe–host interactions. Proc Natl Acad Sci. 2018;115(12):E2706–E2715. doi:10.1073/pnas.1715016115

Shen X-X, Opulente DA, Kominek J, Zhou X, Steenwyk JL, Buh KV, Haase MAB, Wisecaver JH, Wang M, Doering DT, *et al.* Tempo and mode of genome evolution in the budding yeast subphylum. Cell. 2018;175(6):1533–1545.e20. doi:10.1016/j.cell.2018.10.023

Shewmaker F, Mcglinchey RP, Thurber KR, Mcphie P, Dyda F, Tycko R, Wickner RB. The functional curli amyloid is not based on in-register parallel beta-sheet structure. J Biol Chem. 2009;284:25065–25076.

Sievers F, Wilm A, Dineen D, Gibson TJ, Karplus K, Li W, Lopez R, McWilliam H, Remmert M, Söding J, *et al.* Fast, scalable generation of high-quality protein multiple sequence alignments using Clustal Omega. Mol Syst Biol. 2011;7(1):539. doi:10.1038/msb.2011.75

Singh S, Uppuluri P, Mamouei Z, Alqarihi A, Elhassan H, French S, Lockhart SR, Chiller T, Edwards JE, Ibrahim AS. The NDV-3A vaccine protects mice from multidrug resistant Candida auris infection. PLOS Pathog. 2019;15(8):e1007460. doi:10.1371/journal.ppat.1007460

Smukalla S, Caldara M, Pochet N, Beauvais A, Guadagnini S, Yan C, Vinces MD, Jansen A, Prevost MC, Latgé J-P, *et al.* FLO1 is a variable green beard gene that drives biofilm-like cooperation in budding yeast. Cell. 2008;135(4):726–737. doi:10.1016/j.cell.2008.09.037

Srivastava V, Singla RK, Dubey AK. Emerging virulence, drug resistance and future anti-fungal drugs for Candida pathogens. Curr Top Med Chem. 2018;18(9):759–778. doi:10.2174/1568026618666180528121707

Stamatakis A. RAxML version 8: a tool for phylogenetic analysis and post-analysis of large phylogenies. Bioinformatics. 2014;30(9):1312–1313. doi:10.1093/bioinformatics/btu033

Stamler R, Kappé G, Boelens W, Slingsby C. Wrapping the α-crystallin domain fold in a chaperone assembly. J Mol Biol. 2005;353(1):68–79. doi:10.1016/j.jmb.2005.08.025

Steentoft C, Vakhrushev SY, Joshi HJ, Kong Y, Vester-Christensen MB, Schjoldager KT-BG, Lavrsen K, Dabelsteen S, Pedersen NB, Marcos-Silva L, *et al.* Precision mapping of the human O-GalNAc glycoproteome through SimpleCell technology. EMBO J. 2013;32(10):1478–1488. doi:10.1038/emboj.2013.79

Steenwyk JL, Buida TJ, Li Y, Shen X-X, Rokas A. ClipKIT: a multiple sequence alignment trimming software for accurate phylogenomic inference. PLoS Biol. 2020;18(12):e3001007. doi:10.1371/journal.pbio.3001007

Suyama M, Torrents D, Bork P. PAL2NAL: robust conversion of protein sequence alignments into the corresponding codon alignments. Nucleic Acids Res. 2006;34(Web Server):W609–W612. doi:10.1093/nar/gkl315

Teufel F, Almagro Armenteros JJ, Johansen AR, Gíslason MH, Pihl SI, Tsirigos KD, Winther O, Brunak S, von Heijne G, Nielsen H. Signalp 6.0 predicts all five types of signal peptides using protein language models. Nat Biotechnol. 2022;40(7):1023–1025. doi:10.1038/s41587-021-01156-3

Teunissen AW, Steensma HY. Review: the dominant flocculation genes of saccharomyces cerevisiae constitute a new subtelomeric gene family. Yeast. 1995;11(11):1001–1013. doi:10.1002/yea.320111102

Uppuluri P, Lin L, Alqarihi A, Luo G, Youssef EG, Alkhazraji S, Yount NY, Ibrahim BA, Bolaris MA, Edwards JE, *et al.* The Hyr1 protein from the fungus Candida albicans is a cross kingdom immunotherapeutic target for Acinetobacter bacterial infection. PLoS Pathog. 2018;14(5):e1007056. doi:10.1371/journal.ppat.1007056

Verstrepen KJ, Jansen A, Lewitter F, Fink GR. Intragenic tandem repeats generate functional variability. Nat Genet. 2005;37(9):986–990. doi:10.1038/ng1618

Verstrepen KJ, Reynolds TB, Fink GR. Origins of variation in the fungal cell surface. Nat Rev Microbiol. 2004;2(7):533–540. doi:10.1038/nrmicro927

Wang L-G, Lam TT-Y, Xu S, Dai Z, Zhou L, Feng T, Guo P, Dunn CW, Jones BR, Bradley T, *et al.* Treeio: an R package for phylogenetic tree input and output with richly annotated and associated data. Mol Biol Evol. 2020;37(2):599–603. doi:10.1093/molbev/msz240

Wasmer C, Lange A, Van Melckebeke H, Siemer AB, Riek R, Meier BH. Amyloid fibrils of the HET-s(218–289) prion form a beta solenoid with a triangular hydrophobic core. Science. 2008;319(5869):1523–1526. doi:10.1126/science.1151839

Waterhouse AM, Procter JB, Martin DMA, Clamp M, Barton GJ. Jalview version 2—a multiple sequence alignment editor and analysis workbench. Bioinformatics. 2009;25(9):1189–1191. doi:10.1093/bioinformatics/btp033

Welsh RM, Sexton DJ, Forsberg K, Vallabhaneni S, Litvintseva A. Insights into the unique nature of the east Asian clade of the emerging pathogenic yeast Candida auris. J Clin Microbiol. 2019;57(4):e00007–19. doi:10.1128/JCM.00007-19

Wilkins M, Zhang N, Schmid J. Biological roles of protein-coding tandem repeats in the yeast Candida albicans. J Fungi. 2018;4(3):78. doi:10.3390/jof4030078

Willaert R. Adhesins of yeasts: protein structure and interactions. J Fungi. 2018;4(4):119. doi:10.3390/jof4040119

Willbold D, Strodel B, Schröder GF, Hoyer W, Heise H. Amyloid-type protein aggregation and prion-like properties of amyloids. Chem Rev. 2021;121(13):8285–8307. doi:10.1021/acs.chemrev.1c00196

Winter DJ. Rentrez: an R package for the NCBI eUtils API. R J. 2017;9(2):520–526. doi:10.32614/RJ-2017-058

Xie X, Qiu W-G, Lipke PN. Accelerated and adaptive evolution of yeast sexual adhesins. Mol Biol Evol. 2011;28(11):3127–3137. doi:10.1093/molbev/msr145

Xu Z, Green B, Benoit N, Schatz M, Wheelan S, Cormack B. De novo genome assembly of *Candida glabrata* reveals cell wall protein complement and structure of dispersed tandem repeat arrays. Mol Microbiol. 2020;113(6):1209–1224. doi:10.1111/mmi.14488

Xu Z, Green B, Benoit N, Sobel JD, Schatz MC, Wheelan S, Cormack BP. Cell wall protein variation, break-induced replication, and subtelomere dynamics in *Candida glabrata*. Mol Microbiol. 2021;116(1):260–276. doi:10.1111/mmi.14707

Yang Z. Likelihood ratio tests for detecting positive selection and application to primate lysozyme evolution. Mol Biol Evol. 1998;15(5):568–573. doi:10.1093/oxfordjournals.molbev.a025957

Yang Z. PAML 4: phylogenetic analysis by maximum likelihood. Mol Biol Evol. 2007;24(8):1586–1591. doi:10.1093/molbev/msm088

Yang J, Yan R, Roy A, Xu D, Poisson J, Zhang Y. The I-TASSER suite: protein structure and function prediction. Nat Methods. 2015;12(1):7–8. doi:10.1038/nmeth.3213

Yu G. Using ggtree to visualize data on tree-like structures. Curr Protoc Bioinforma. 2020;69(1):e96. doi:10.1002/cpbi.96

Zhang J. Evolution by gene duplication: an update. Trends Ecol Evol. 2003;18(6):292–298. doi:10.1016/S0169-5347(03)00033-8

Zhang J, Nielsen R, Yang Z. Evaluation of an improved branch-site likelihood method for detecting positive selection at the molecular level. Mol Biol Evol. 2005;22(12):2472–2479. doi:10.1093/molbev/msi237

Zhao X, Oh S-H, Coleman DA, Hoyer LL. *ALS51*, a newly discovered gene in the *Candida albicans* ALS family, created by intergenic recombination: analysis of the gene and protein, and implications for evolution of microbial gene families. FEMS Immunol Med Microbiol. 2011;61(3):245–257. doi:10.1111/j.1574-695X.2010.00769.x

Editor: A. Mitchell